Canadian Science Publishing | Canadian Geotechnical Journal

Longevity of Twelve Geomembranes in Chlorinated Water

Journal:	*Canadian Geotechnical Journal*
Manuscript ID	cgj-2019-0520.R2
Manuscript Type:	Article
Date Submitted by the Author:	25-Apr-2020
Complete List of Authors:	Morsy, Mohamed; Queen's University, Civil Engineering; Ain Shams University, Structural engineering Rowe, R. Kerry; Queen's University, Civil Engineering Abdelaal, Fady; Queen's University, Civil Engineering
Keyword:	Geomembranes, Chlorinated water, HDPE, LLDPE, Ageing
Is the invited manuscript for consideration in a Special Issue? :	Not applicable (regular submission)

Longevity of Twelve Geomembranes in Chlorinated Water

M.S. Morsy, R. Kerry Rowe* and F.B. Abdelaal

Abstract

The long-term performance of geomembranes with twelve different resin/antioxidant master-batch combinations, including eight HDPE, three linear low density polyethylene (LLDPE), and one blended polyolefin (BPO) base resins, is investigated. Results are reported for immersion tests in chlorinated water (0.5 ppm) for 35 months at 85°C. The degradation trends show that the choice of resin type played a key role in the longevity of the geomembranes but also that some hindered amine light stabilizer (HALS) packages contributed to better resistance to degradation in chlorinated water. The results show that the specific antioxidant package is more important than the initial oxidative induction time (OIT) in terms of long-term performance. Finally, it is shown that while increased thickness may be beneficial, a more resistant resin or antioxidant/stabilizes package can be more effective than increasing thickness in improving geomembrane performance in chlorinated water. The conclusion regarding the beneficial role of HALS is specific to chlorinated water and generally is not true in other cases of submerged or buried geomembranes.

Keywords: Geosynthetics, Geomembranes, Chlorinated water; Oxidative degradation; HDPE; LLDPE; Blended polyolefin; Ageing; Antioxidants.

[1] PhD. Student, GeoEngineering Centre at Queen's-RMC, Queen's University, Kingston ON, Canada, K7L 3N6. Email: mmorsy@queensu.ca

[2] Barrington Batchelor Distinguished University Professor and Canada Research Chair in Geotechnical and Geoenvironmental Engineering, GeoEngineering Centre at Queen's-RMC, Queen's University, Ellis Hall, Kingston ON, Canada K7L 3N6. E-mail: kerry.rowe@queensu.ca, Phone: (613) 533-3113. Fax: (613) 533-2128.

[3] Assistant Professor, GeoEngineering Centre at Queen's-RMC, Queen's University, Ellis Hall, Kingston ON, Canada K7L 3N6. E-mail: fady.abdelaal@queensu.ca

* Corresponding Author.

1 Introduction

Geotechnical and geoenvironmental engineers frequently use polyethylene (PE) geomembranes (GMBs) in applications including landfills, brine ponds, mining facilities, stormwater ponds, and potable water reservoirs for containment of liquids and gases, and to retard diffusion of many ions and compounds (Rowe et al. 2004). Many factors affect the performance of the geomembrane including diffusion (Rowe 1998, 2005; Sangam and Rowe 2001; 2005; Joo 2004; McWatters and Rowe 2009, 2010, 2015; Mendes et al. 2013; Eun et al. 2014; Jones and Rowe 2016; Saheli et al. 2016; Saheli and Rowe 2016; Rowe et al. 2016a&b), leakage and contaminant transport (Rowe and Booker 1995; Rowe 1988, 1998, 2005, 2012, 2018, 2020; Touze et al. 1999), temperature (e.g., Rowe and Sangam 2002; Yoshida and Rowe 2003; Rowe and Arnepalli 2008; Rowe et al. 2009; Rowe and Hoor 2009; Rowe and Islam 2009; Rowe 2012; Ewais et al. 2018; Morsy and Rowe 2017a; Awad et al. 2018; Morsy and Rowe 2020), exposure to the elements (e.g., Sangam and Rowe 2002; Rowe et al 2003; Take et al. 2007, 2012, 2015; Rowe et al 2012a&b; Rowe and Ewais 2015), tensile strains (Tognon et al. 2000, Eldesouky and Brachman 2018; Rowe and Yu 2019), and chemical exposure (e.g., Rowe et al. 2008; Abdelaal et al. 2014; Rowe and Abdelaal 2016; Morsy and Rowe 2017b; Abdelaal and Rowe 2017; Tian et al. 2017, 2018; Morsy et al. 2019; Rowe et al. 2019a). The focus of this paper is on the last of these, chemical exposure, and the effect of chlorinated water the performance of 12 different geomembranes.

GMBs are used as base liners in potable water reservoirs for containment of drinking water with 0.2-1 ppm free chlorine added to disinfect pathogenic micro-organisms harmful to human health such as fungi, viruses, and bacteria (Kim et al. 2002; Eng et al. 2011). Chlorine is one of the halogen group VII elements that is characterized by small atomic radii, high electron affinities, and high electronegativities (Lundbäck 2005), thus chlorine is a very strong oxidizing agent (Fair et al. 1948, Yu et al. 2011). With a few notable exceptions mentioned below, there is a paucity published data related to the performance of GMBs exposed to chlorinated water. Mills (2011) reported the formation of cracks in the side of a 1 mm thermoplastic olefin GMB exposed to water in a potable water reservoir just six months after installation. Other studies

examining the performance of GMBs exposed to chlorinated water reported that the antioxidant depletion rate in chlorinated water was fast relative to other incubation fluids such as water without chlorine, municipal solid waste leachate with surfactant, and mining heap leach pads solutions (Abdelaal and Rowe 2014; Morsy et al. 2016, Morsy and Rowe 2017b, Abdelaal and Rowe 2019, Abdelaal et al. 2019).

Abdelaal and Rowe (2019) and Abdelaal et al. (2019) investigated the performance of two high density polyethylene (HDPE) GMBs immersed in chlorinated water (Figure 1). The two GMBs were produced by the same manufacturer but from different polymer resins. One GMB did not contain hindered amine light stabilizers (HALS) (MxA15-Figure 1a; Abdelaal and Rowe 2019) while the other (MxC15-Figure 1b; Abdelaal et al. 2019) was stabilized with HALS. The two studies showed substantial difference between the degradation of the two HDPE GMBs although they showed more similar performance when immersed in other incubation media (municipal solid waste, leachate, and brine). Therefore, it was concluded that chlorinated water was responsible for the difference in degradation mechanism exhibited by MxC15 (Figure 1). However, it was not clear whether the difference in resin or the HALS in MxC15 had the dominant effect on the superior performance of MxC15 over MxA15.

Following from the foregoing, the primary objective of this study is to investigate the role of resin (e.g., as manifest by different resin types and densities) and antioxidant package (especially the presence or absence of HALS) on the degradation of different PE GMBs in chlorinated water. Previous studies have shown that are GMB with a given antioxidant package may be well-suited for one solution may not be well-suited for another solution with a different chemical composition of pH (Abdelaal et al. 2014; Morsy and Rowe 2017b; Morsy et al. 2019). To build on this prior finding, this paper examines 12 different geomembranes from three manufacturers, and compares the performance of different products with the objective of demonstrating that GMBs with either different resins or antioxidant packages produced by the same manufacturer can perform very differently under the same testing conditions. In doing so, it also seeks to highlight critical role played by the different antioxidant packages used in the different products.

2 Experimental Investigation

2.1 GMBs examined

The twelve commercially available smooth GMBs investigated in this study included: eight HDPE, three linear low density (LLDPE), and one blended polyolefin (BPO) GMB. In the generic naming convention for each GMB, the first letter denotes the resin type by "M" for medium density polyethylene (MDPE), "L" for LLDPE, and "B" for a (secret) blend of polyolefin resins (BPO). The second letter identifies the three different manufacturers denoted generically by x, y, and z. The third letter (e.g., A, C, D, E, F1, F2, F3, & V) designates the specific GMB, each with either a different resins and/or antioxidant package, while the last number in the name indicates the GMB nominal thickness (e.g., 15= 1.5 mm, 20= 2.0 mm, and 30 = 3.0mm). Five GMBs were produced by manufacturer "x" (viz, MxC15, MxV30, LxD15, LxE15, and LxV20), another five GMBs were produced by manufacturer "y" (viz: MyF1-15, MyF2-15, MyF3-15, MyE15, and MyEW15), and two GMBs were produced by manufacturer "z" (viz: MzV20 and BzV20). All the HDPE GMBs investigated in this study were produced from medium density polyethylene (MDPE) polymer resin with the addition of 2-3% carbon black (by weight) to the polymer resin increasing the GMB density into the HDPE range ($\geq$ 0.941 g/cm^3; ASTM 2011). All the GMBs in this study were blown film using a circular die except for MyF3-15 that was manufactured using a flat die (the different dyes require resins with a different molecular weight distributions). Except for LxD15, all the GMBs were inferred to be stabilized with HALS given their relatively high HP-OIT values (>500 minutes; Scheirs 2009). However, LxD15's manufacturer indicated the presence of traces of HALS during the manufacturing of this GMB (Abdelaal et al. 2012). The different types of GMBs examined in this study will allow the comparison between their relative GMB performance and longevity in chlorinated water.

To allow convenient examination of the effect of different variables on GMB resistance to chlorine, the twelve GMBs examined for the first time in this study were divided into four groups (Tables 1):

Group 1 GMBs (Table 1a) were used to investigate the effect of resin and role of HALS on the performance of GMBs in chlorinated water;

Group 2 GMBs (Table 1b) were used to investigate the effect of initial OIT value on the OIT depletion time and longevity of GMBs in chlorinated water;

Group 3 (Table 1c) was used to investigate the effect of GMB's resin density on its resistance to degradation; and

Group 4 (Table 1d) was used to investigate the effect of GMB's thickness on the longevity of GMBs in chlorinated water.

In some cases a GMB was used in more than one group if including it aided in the assessment of the GMB characteristic being evaluated.

2.2 Accelerated ageing and incubation media

GMB coupons with dimensions of 190×95 mm were immersed in 4-liter glass jars filled with chlorinated water (pH= 9.9±0.13). The GMB coupons were separated by 5 mm diameter glass rods to ensure the exposure of GMBs to chlorinated water from both sides. The immersion tests were conducted only at 85^{o}C to accelerate the ageing of the twelve GMBs to aid the comparison between their degradation in reasonable time. Chlorinated water was prepared by mixing 5 mg/l of sodium hypochlorite (laboratory grade 5.65-6%) with deionized water.

Rapid depletion of free chlorine (in less than 2 hours) was observed (Abdelaal and Rowe 2014; Abdelaal and Rowe 2019) when using an initial chlorine concentration of 0.5 ppm due to the large surface area of GMB coupons compared to the available free chlorine in the 4-liter jars. To overcome the rapid consumption of chlorine, continuous injection techniques have been used in the pipe literature to maintain the free chlorine content and pH at constant levels at elevated temperatures. However, this technique does not simulate GMB liners in potable water reservoirs that are exposed to repeated spikes of high chlorine concentration over their service life. Abdelaal and Rowe (2019) immersed a 3 cm× 1.8 cm GMB coupon in a 3.5L of water with 1 ppm free chlorine solution (a typical mass loading in the field) and showed that it exhibited the same behaviour as 16 coupons (20 × 10 cm) immersed in 3.5 L of water with free boosted

chlorine 600 –fold times to simulating the same mass of chlorine per unit GMB surface area as in the first experiment. Therefore, the concentration of free chlorine in the jars was boosted to 600 ppm to simulate the mass loading as in a typical pond and allow the use of enough coupons to test the GMBs over the entire duration of this study. The solution was refreshed every 10 days to simulate spikes in concentrations that are typical for potable water reservoirs and to overcome the consumption of free chlorine by evaporation and chemical interaction with antioxidants (Abdelaal and Rowe 2019).

2.3 Index Properties

A series of index tests were performed to estimate the initial properties of the GMBs (Table 1) and to monitor the ageing of GMBs after immersion in chlorinated water. These index tests established the change in Std-OIT, HP-OIT, high load melt flow index (HLMI), and tensile break properties with time using standard ASTM tests (see Supplemental Material for more details).

3 Degradation Trend for the Examined GMBs in Chlorinated Water

The traditional oxidative degradation trend of GMBs reported by Hsuan and Koerner (1998) involves three stages of degradation until the nominal failure of a certain mechanical property is reached. Stage (I) involves the antioxidant/stabilizer depletion, then the GMB experiences an induction period (Stage II) until the onset of Stage (III) that ends by reaching nominal failure, t_{NF}, commonly defined as when there has been 50% loss of: (a) the initial property of the GMB or that specified by GRI-GM13 (Rowe et al. 2009), or (b) the SCR equilibrium value after physical ageing (Rowe et al. 2019b; Morsy and Rowe 2020). This degradation trend was observed for the GMB MxA15 (without HALS; Figure 1a; Abdelaal and Rowe 2019) when immersed in chlorinated water. On the contrary, Abdelaal et al. (2019) suggested different oxidative degradation trend for the GMB (MxC15; Figure 1b) stabilized with HALS when immersed in chlorinated water. The degradation occurred in two stages, the first stage (Stage A) involves early time surface degradation induced initial reduction (before full depletion of OIT either Std-OIT or HP-OIT) in the tensile break properties and SCR to a stabilized value denoted by $F_{b\text{-}so}$ (stabilized break strength), $\varepsilon_{b\text{-}so}$ (stabilized break strain), and SCR_{so} (stabilized SCR). These properties were retained for a relative long time, followed

by rapid degradation to nominal failure and severe degradation designated as degradation Stage B. The time to severe degradation was introduced by Abdelaal et al. (2019) to describe the longevity of GMBs in potable water reservoirs as the time at which the GMB is about to completely lose its mechanical properties, and reached when SCR has reduced to 50 hours, and tensile break strain has reduced to about 5% of the unaged GMB break strain.

There was a clear difference in the performance of the two GMBs (MxA15 and MxC15), however, it was not clear whether this difference was due to a difference in resin or the antioxidant package (especially HALS). To obtain some insight into this question, the longevity of both MxA15 and MxC15 is discussed in detail and compared to the degradation trend/performance of additional 11 GMBs with different antioxidant/stabilizer packages, resins (density), and thicknesses.

GMB MxA15 (Resin M1; no HALS; Figure 1a) followed the traditional degradation model (Hsuan and Koerner 1998) in that there is no change in SCR until Std-OIT was fully depleted. However, degradation in SCR began before full depletion of the HP-OIT, and indeed the traditional time to nominal failure, t_{NF}, corresponds to a 50% reduction in SCR was about 2.9 months, whereas it took about 5.6 months before HP-OIT had depleted to a residual value. In this case, there was severe degradation (t_{sd}) of the GMB at 4 months and the specimen was completely brittle at 5.6 months when the HP-OIT had just depleted to a small residual value (8 minutes).

In contrast, for MxC15 (Resin M2-1with HALS; Figure 1b) SCR decreased to SCR_{so} equaled $0.65 \cdot SCR_o$ ($\pm 0.15 \cdot SCR_o$) in less than 5.8 months before either Std-OIT or HP-OIT had depleted to a residual value (Stage A; Figure 1b). However, SCR remained at $SCR_{SO} = 0.65 \cdot SCR_o$ for about 30 months after both Std-OIT and HP-OIT had depleted. In this case the HP-OIT residual value was quite high ($HP\text{-}OIT_r = 0.53 \cdot HP\text{-}OIT_o$). After about 36 months the SCR entered what is referred to here as Stage B and began to decrease again, reaching the traditional t_{NF} (50% of SCR_o) at ~ 39 months. Severe degradation was evident at t_{sd} ~58 months (14-fold longer than for MxA15).

In this paper, tensile break properties are used to monitor the degradation of the GMBs because: (i) the tensile test considers oxidation of both GMB surfaces while the SCR mitigates the effect of one of the two oxidized surfaces due to the prescribed notch, (b) the very high SCR of some GMBs (up to 37,000 hours or 4.2 years; Table 1) made it impractical to continuously monitor SCR until severe degradation (t_{sd}), and (c) to mitigate the effect of physical ageing observed in SCR results (Ewais and Rowe 2014; Rowe et al. 2019b; Morsy and Rowe 2020). Although Abdelaal and Rowe (2019) only monitored SCR to assess the longevity of MxA15, its degradation time will be also compared to those obtained in the current study and hence it was assumed that the t_{sd} in SCR and tensile break strain are reached at similar times. This assumption was made based on the observation, reported in Abdelaal et al. (2019), that t_{sd} obtained from both tensile break strain and the SCR of MxC15 were close when immersed in the same chlorinated water as examined in the current study.

The degradation trend of the new 11 GMBs investigated in this study (Figure 2) was similar to that of the GMB MxC15 (Figure 2g; examined by Abdelaal et al. 2019). All the GMBs examined showed a gradual reduction in the tensile break properties immediately after incubation (Stage A; Figures 2a to 2h). For all GMBs examined, the average normalized Stage A plateau value for break strength was $0.64 \leq F_{b\text{-}SO}/F_{bo} \leq 0.84$ and break strain was $0.66 \leq \varepsilon_{b\text{-}SO} / \varepsilon_{bo} \leq 0.90$ (Table 2). The fact that degradation in the tensile properties in Stage A started before full depletion of antioxidants/stabilizers detected by either the Std-OIT or HP-OIT tests is attributed to their rapid depletion at the surface followed by extensive degradation of the GMB's surface which reduced the tensile properties while the GMB core was still stabilized with antioxidants (Abdelaal et al. 2019).

Over the almost 3 years of testing undertaken for this paper, four GMBs examined here (MyF3-15, MyE15, MyEW15, and LxD15) as well as MxA15 (Abdelaal and Rowe 2019), exhibited a second stage degradation (denoted as Stage B) until t_{sd} was approached or in some cases, was reached (Figures 1a and 2i to 2l). Of these five GMBs, four were made of four different MDPE resins (M1, M6, M7, and M8) and one LLDPE resin (L1). Also out of these five, three (MyEW15, MyF3-15 and MyE15) were stabilized with

HALS and two had either very little (LxD15) or no (MxA15) HALS. The t_{sd} for tensile break strain of the four GMBs was 15.4 months (Figure 2i; MyEW15; resin M8), 22.1 months (Figure 2j; MyF3-15; resin M6), 29 months (Figure 2k; MyE15; resin M7), and 49 months (extrapolated; Figure 2l; LxD15; resin L1). All were significantly longer than the 4 months (based on SCR) reported for MxA15 (Resin M1-without HALS; Abdelaal and Rowe 2019). Thus, the shortest t_{sd} observed in the current study (15.4 months; Figure 2i; MyEW15: Resin M8) was ~4 fold higher than MxA15 (4 months; Figure 1a; resin M1; Abdelaal and Rowe 2019).

Eight GMBs did not reach Stage B during the 35 months of incubation, three (MxV30, MxC15, and MzV20; Figures 2f-h) were made from the same nominal MDPE resin (M2), two (MyF1-15 and MyF2-15; Figures 2a & b) were other MDPE resins (M4 and M5), two (LxE15 and LxV20; Figures 2c & d) were LLDPE resins (L1 and L2) and one (BzV20; Figure 2e) was a BPO resin (B2).

The results presented in the previous two paragraphs indicate that four of the MDPE had poorer performance than two LLDPE and one BPO but that, conversely, four MDPE performed better than one LLDPE. This suggest that the specific resin played a significant role in terms of the resistance to degradation in chlorinated water but that one cannot draw a simple generalization about the longevity of MDPE, LLDPE and BPO resins; performance depends on the specific combination of resin and antioxidant/stabilizer package. Of the multiple products with nominally the same base resins (although different antioxidant packages), three (MxC15, MzV20 and MxV30), with the same nominal MDPE resin (M2), remained in Stage A for the 35-month testing period (Figure 2f-h). Of two products with the same LLDPE resin, L1, one (LxE15; Figure 2c) remained in Stage A for the full 35 months examined while the other (LxD15; Figure 2l) entered Stage B and began to degrade after 28 months with an inferred t_{sd} ~ 49 months. This raises the questions why the difference in behaviour?

3.1 Role of HALS and resin in degradation trend of GMBS in chlorinated water

The effect of the type of polymer resin and the role of HALS on the performance of GMBs in chlorinated water was examined by monitoring four new GMBs (two HDPE GMBs and two LLDPE) and one GMB

previously studied by Abdelaal and Rowe (2019). These five GMBs were designated herein as Group 1 GMBs and had properties summarized in Table 1a.

3.1.1 Role of HALS in GMB performance in chlorinated water

The role of HALS can be best inferred from the relative performance of LxD15 (Figure 2l) and LxE15 (Figure 2c). LxD15, which exhibited Stage B degradation, was produced using the same nominal resin (L1) of LxE15 which remained in Stage A. The main difference between LxD15 and LxE15 was the low initial HP-OIT (350±13 min.) value for LxD15 and the low residual HP-OIT values reached at the end of the incubation ($0.07 \cdot HP\text{-}OIT_o$). Both imply that HALS was not a significant part of LxD15's antioxidant package and the trace amount of HALS was insufficient to be effective. This implies that HALS had a role in delaying the degradation of LxE15. This, together with the comparison made in Figure 1 between MxA15 (no HALS; Abdelaal and Rowe 2019) and MxC15 (with HALS) suggested a role for HALS in providing some protection to GMBs resins from chlorinated water.

3.1.2 Role of resin in chlorinated water

To focus on the role of the resin, consider the relative performance of MyEW15 and MyE15 (Table 1a) produced in the same year by the same manufacturer using two different polymer resins evident from the 3-fold difference in initial SCR between MyE15 (~13,000 hours) and MyEW15 (~4500 hours) and 2-fold difference in melt flow ratio of MyE15 (123) compared to MyEW15 (67). Although the two antioxidant/stabilizer packages had different concentration as implied by their initial Std-OIT and HP-OIT values, the Std-OIT depletion times (1.9 and 2.0 months for MyEW15 and MyE15, respectively; Table 3) and HP-OIT depletion times (4.0 and 4.7 months, for MyEW15 and MyE15 respectively; Table 4) were quite similar. The latter is especially notable since MyE15 had almost twice the initial HP-OIT as MyEW15 but only took an extra 0.7 months (17%) longer to deplete. Thus, the resins of the two GMBs were left similarly unprotected (with normalized residual $HP\text{-}OIT_r$= 0.30 for MyEW15 and 0.39 for MyE15) from oxidation after OIT depletion. The two GMBs exhibited similar reduction in tensile break strain in Stage A, reaching a normalized value of $\varepsilon_{b\text{-}SO}$ of $0.79 \cdot \varepsilon_{bo}$ for MyEW15 and $0.76 \cdot \varepsilon_{bo}$ for MyE15. For MyEW15

(resin M8), Stage B started after 10 months of incubation (i.e., 6 months after HP-OIT reached residual value; Figure 2i) and t_{sd} was reached at 15.4 months with the normalized tensile break strain as low as $0.075 \cdot \varepsilon_{bo}$ after 16 months. In contrast, for MyE15 (resin M7), Stage B started after 16 months (i.e., 11.3 months after HP-OIT reached a residual value; Figure 2k) and normalized break strain reached $0.51 \cdot \varepsilon_{bo}$ after 22 months. The estimated t_{sd} for break strain was ~15.4 months for MyEW15 and ~29 months for MyE15 (i.e., a 2-fold difference).

The longer time for the onset of Stage B and the slower degradation rate of tensile break strain in Stage B of MyE15 compared to MyEW15 is considered most likely due to the better performance of the polymer resin of MyE15 than that of MyEW15 in chlorinated water. However, despite the similar normalized values of $HP\text{-}OIT_r/HP\text{-}OIT_o$, there was a 2.5-fold difference in $HP\text{-}OIT_r$ of MyE15 (520 minutes) compared to MyEW15 (200 minutes) that deserves comment. While the resin is considered to be the primary difference affecting t_{sd}, the possibility that the high $HP\text{-}OIT_r$ for MyE15 may have contributed to its resistance to degradation cannot be excluded. Since the specific chemistry of the two antioxidant/stabilizer packages remains confidential to the manufacturer, it is possible that the higher $HP\text{-}OIT_r$ implies more HALS in the core of MyE15 which may have also contributed to impeding the interaction of the chlorine reactive species with the GMB. Notwithstanding this acknowledged uncertainty, the resin is considered the primary factor influencing t_{sd} because: (i) the $HP\text{-}OIT_r$ = 520 minutes for MyE15 was very similar to the 500 minutes for MyF3-15 which entered Stage B later and degraded faster, and (ii) LxE15 with a $HP\text{-}OIT_r$ (160 minutes), lower than either MyEW15 (200 minutes) or MyE15 (520 minutes), never entered Stage B in 35 months of testing while MyEW15 (200 minutes) entered Stage B at 10 months and MyE15 (520 minutes) at 16 months. The role of resin and antioxidant package is explored in more detail in the next section.

4 Factors affecting the longevity of 12 GMBs examined in Chlorinated Water

The effect of HP-OIT antioxidant/stabilizer package and resin was illustrated by the degradation trends for GMBs in chlorinated water shown in Figure 2 and briefly discussed in Section 3.1 to illustrate the role of

resin and HALS. This section provides a more detailed discussion of the differences between the antioxidant packages and resins of the 12 GMBs examined herein based on their index values and resin characteristics, and their effect on the longevity of the GMBs examined when exposed to chlorinated water. To allow convenient examination of the effect of different variables on resistance to chlorine the geomembranes were divided (GMB groups 2, 3, & 4; Tables 1b, c, & d).

4.1 Effect of initial OIT

The effect of initial OIT value (Std-OIT and HP-OIT) on the antioxidant depletion times and longevity of GMBs is examined through a comparison between the relative performances of six GMBs designated as Group 2 GMB with properties given in Table 1b. These GMBs were selected such that they had the same thickness (1.5 mm) and similar density so that the primary difference was the antioxidant package and initial OIT values. This group involves two sets of GMBs: Set #1 includes HDPE GMBs (MyF1-15, MyF2-15, MyF3-15, and MyE15), and Set #2 includes two LLDPE GMBs (LxD15 and LxE15). The four HDPE GMBs were made of different resins as implied by the different MFI and SCR values. The flat die MyF3-15 had an initial melt flow ratio (MFR) 20% of that for the other three blown film HDPE GMBs. This comparison is directed at answering the two questions:

(1) does a higher initial OIT value imply a longer antioxidant depletion time?

(2) does a higher initial OIT value, especially HP-OIT, results in longer t_{sd}?

Does a higher initial OIT value imply a longer antioxidant depletion time?

The Std-OIT results (Figure 3) were modeled using a two-parameter (first order) exponential decay function to describe the depletion in OIT with incubation time, viz:

$$OIT_t = OIT_o \times \mathrm{e}^{-st} \quad (1)$$

Taking the natural logarithm on both sides, Equation (1) becomes

$$\ln(OIT_t) = \ln(OIT_o) - st \quad (2)$$

where, OIT_t (minute)= OIT value after incubation time t; OIT_o (minute)= initial OIT value; and s (month^{-1}) = antioxidant depletion rate.

The Std-OIT depletion times for Set #1 GMBs were 3.3 months for MyF3-15 ($Std\text{-}OIT_o$= 210 minutes), 2.5 months for MyF2-15 ($Std\text{-}OIT_o$= 190 minutes), 2.0 months for MyE15 ($Std\text{-}OIT_o$= 150 minutes), and 1.7 months for MyF1-15 ($Std\text{-}OIT_o$= 160 minutes) (Figure 3a and Table 3). Although the longest Std-OIT depletion time was for MyF3-15 with the highest $Std\text{-}OIT_o$, followed by MyF2-15 (second highest $Std\text{-}OIT_o$), this was not the case for MyE15 that had longer depletion times than MyF1-15 with a higher $Std\text{-}OIT_o$. Therefore, a higher initial Std-OIT did not necessarily result in longer Std-OIT depletion time for HDPE GMBs. Furthermore, for Set #2 GMBs (Figure 3b and Table 3), LxD15 had higher $Std\text{-}OIT_o$ (190 minutes) but its depletion time of 3.6 months was less than 4.2 months for LxE15 ($Std\text{-}OIT_o$= 155 minutes). Also, the depletion times for the two LLDPE GMBs in Set #2 were longer than for any of the HDPE GMBs in Set #1. Thus, for the four HDPEs in Set #1 and the two LLDPEs in Set #2, there was no clear relationship between the initial Std-OIT value and depletion times.

The HP-OIT of all the examined GMBs depleted to high residual values, hence a three parameters exponential decay model was used to describe the depletion of HP-OIT with time, viz:

$$OIT_t = \{(OIT_o - OIT_r) \times e^{-st}\} + OIT_r \quad (3)$$

where, OIT_t (minute) is the HP-OIT value at any time $\{t, (\text{month})\}$, OIT_r (minute) is the residual HP-OIT value, OIT_o (minute) is the initial HP-OIT value, and s (month^{-1}) is the HP-OIT depletion rate.

The HP-OIT depletion time was 9.3 months for MyF1-15 ($HP\text{-}OIT_o$= 1100 minutes; OIT_r = 350 minutes; normalized OIT_r= 0.32), 8.2 months for MyF2-15 ($HP\text{-}OIT_o$= 780 minutes; OIT_r = 400 minutes; normalized OIT_r = 0.51), 7.0 months for MyF3-15 ($HP\text{-}OIT_o$= 1300 minutes; OIT_r = 500 minutes; normalized OIT_r = 0.38), and 4.7 months for MyE15 ($HP\text{-}OIT_o$= 1300 minutes; OIT_r = 520 minutes; normalized OIT_r=0.39). Thus although MyF3-15 and MyE15 had the highest initial $HP\text{-}OIT_o$ and residual $HP\text{-}OIT_r$ values (Table 4 and Figure S1; see supplementary material), they had the shortest time to

depletion. For the LLDPE GMBs, the depletion time was 7.9 months for LxD15 ($HP\text{-}OIT_o$= 350 minutes; OIT_r = 25 minutes; normalized OIT_r=0.07) and 5.8 months for LxE15 ($HP\text{-}OIT_o$= 890 minutes; OIT_r = 160 minutes; normalized OIT_r=0.18) (Table 4 and Figure S1). Thus, the results showed no relationship between the $HP\text{-}OIT_o$ values or the $HP\text{-}OIT_r$ values and the depletion times for both sets of GMBs.

The forgoing implies that the answer to the first questions posed above is that a higher initial OIT value does not necessarily imply a longer antioxidant depletion time; the nature of the antioxidant is more important than the initial value. This is because the initial OIT value only represents the initial concentration of antioxidants not their resistance to depletion or extraction. For instance, adding the same concentration of Irganox 1010 or Irganox 1330 to the polymer resin results in the same initial Std-OIT, but Irganox 1010 is likely to give a greater antioxidant depletion time than Irganox 1330 due to its higher molecular weight (Ewais et al. 2014). This does not exclude the likelihood that, for the same antioxidant/stabilizer package, higher OIT may extend the time to depletion up to the point where the GMB is saturated and excess OIT blooms out quickly.

Does a higher initial OIT value, especially HP-OIT, results in longer t_{sd}?

Changes in MFI (Figures 4a and b) were observed after 2-month immersion for MyF3-15 (implying cross-linking reactions), 10-22 months for MyF1-15 (also cross-linking reactions ignoring the anomalous point at 6 months), 10 months for LxD15 and LxE15 and 10-20 months for MyE15 (implying chain scission reactions), and 22-35 months for MyF2-15 (chain scission reactions; although the change is small). The results of the MFI might not give a clear evidence for the onset time of the oxidation reaction because chain scission and cross linking reactions might occur simultaneously resulting in no net change in the normalized MFI value but a reduction in tensile break properties could be observed beforehand as observed for all the GMBs examined in this section except MyF3-15, and, hence the effect of initial OIT value on the degradation of GMBs cannot be judged by MFI alone.

There was no apparent relationship between the initial OIT and the extent of degradation in tensile properties in Stage A as implied from the values of $F_{b\text{-}so}$ and $\varepsilon_{b\text{-}SO}$. For example, MyF1-15 had higher *Std-OIT*$_o$ and lower *HP-OIT*$_o$ compared to MyE15 but they had almost the same amount of degradation in Stage A as indicated by the almost equal normalized values of $\varepsilon_{b\text{-}SO}$ of $0.76\cdot\varepsilon_{bo}$ for MyE15 and MyF1-15 (Figure 5a). Furthermore, an analysis of variance (ANOVA one-way test) showed that the difference between the mean values of normalized $F_{b\text{-}SO}$ for GMBs MyF1-15, MyF3-15, and MyE-15 (0.73, 0.75, and 0.73, respectively; Table 2) was not statistically significant, while the difference between the mean normalized $F_{b\text{-}SO}$ values of MyF2-15 (0.64) and each of MyF3-15 (0.75) and MyE15 (0.73) was statistically significant. Also, the difference between the normalized mean values of $\varepsilon_{b\text{-}SO}$ was not statistically significant except for the difference between the mean normalized values of $\varepsilon_{b\text{-}SO}$ of MyF2-15 and MyF3-15 ($0.70\cdot\varepsilon_{bo}$ and $0.90\cdot\varepsilon_{bo}$, respectively; Table 2). For the LLDPE GMBs, the difference between the mean normalized values of $F_{b\text{-}SO}$ and $\varepsilon_{b\text{-}SO}$ was not statistically significant (Figure 5b) based on the Student t-test (at 95% confidence interval level). Thus, initial OIT values did not affect stabilized values of tensile break properties in Stage A.

Longer OIT depletion time and/or higher initial OIT values did not result in achieving longer t_{sd}. For instance, MyF3-15 had a longer Std-OIT depletion compared to the other three Set #1 HDPE GMBs but it had the shortest t_{sd}. MyF3-15 and MyE-15 had the highest initial HP-OIT amongst the Set #1 HDPE GMBs studied and they were the only two GMBs to encounter degradation in Stage B. Also, there was no relationship between the extent of degradation in Stage A represented by normalized $F_{b\text{-}SO}$ and $\varepsilon_{b\text{-}SO}$ and the t_{sd} as implied by the shortest t_{sd} achieved by MyF3-15 that had the highest normalized $F_{b\text{-}SO}$ and $\varepsilon_{b\text{-}SO}$ amongst the Set #1 HDPE GMBs (Table 2). Furthermore, there was no relationship between the onset time of Stage B and the t_{sd}. For example, Stage B of MyE15 started 4 months before MyF3-15, but the t_{sd} of tensile break strain properties was 29 months for MyE15 (extrapolated t_{sd}) and 22.1 months for MyF3-15 (observed t_{sd}) (Table 2). Thus, for those GMBs that entered Stage B, later onset of Stage B did not necessarily result in longer t_{sd}.

The relative performance of the LLDPE GMBs LxD15 (with traces of HALS) and LxE15 (stabilized with HALS) indicated more severe chain scission oxidation reactions for LxD15 (maximum normalized HLMI=21.64 at 22 months; Figure 4b) compared to LxE15 (maximum normalized HLMI=2.89 at 22 months; Figure 4b). Stage B was observed after 24 months of incubation for LxD15, while LxE15 did not reach the onset of Stage B during 35-month incubation (Figure 5b). While LxD15 and LxE15 are nominally from the same resin, the less degradation encountered by LxE15 compared to LxD15 suggests that the HALS acted as a physical filler/barrier inside the amorphous zone of the GMB that resulted in limiting the oxidation of the amorphous zone, supporting the hypothesis proposed by Abdelaal et al. (2019).

It follows for the foregoing that the answer to the second question posed above is: a higher initial OIT value does not necessarily result in a longer t_{sd}. For given exposure condition, it is the resin that controls the time to severe degradation following the antioxidant depletion. This does not exclude the likelihood for the same resin and exposure conditions, and with the caveats offered in answer to question one, a higher OIT may imply a longer t_{sd}.

4.2 Effect of resin of different density (MDPE, LLDPE and BPO)

It has been documented in the literature (e.g., Scheirs 2009) that a GMB with higher crystallinity will most likely have higher chemical resistance to oxidative degradation when exposed to chemicals and hence HDPE GMBs are expected to have higher chemical resistance than lower crystallinity GMBs such as LLDPE GMBs. In this section, the relative performance of two HDPE (MDPE resin; crystallinity = 53%), one BPO (crystallinity = 50%), and two LLDPE GMBs (crystallinity = 41%). These five GMBs were designated as Group 3 GMBs and had properties as indicated in Table 1c. The relative performance of these five GMBs were compared to investigate whether higher density/crystallinity GMBs do necessarily have better resistance to degradation by chlorinated water than their lower density counterparts or if the antioxidants package plays a key role in providing better performance to GMBs with less density/crystallinity.

LxE15 and MxC15 had very similar initial Std-OIT values (155 and 160 minutes respectively), but the depletion rate was 0.88 month^{-1} for LxE15 and 2.65 month^{-1} for MxC15 (Table 3). This resulted in a depletion time for MxC15 of 1.9 month compared to 4.3 months for LxE15 (Figure 6a). This implies that a similar initial Std-OIT values does not necessarily mean that the chemical composition of the antioxidants is identical, but it indicates that the combination of chemical compounds comprising the antioxidant package of an unaged GMB oxidize at about the same time in the Std-OIT test. Later when the GMB is immersed in a chemical solution, different depletion times were obtained due to the difference in chemical reactions between the incubation fluid and the chemical compounds forming each antioxidant package. For the 2.0 mm GMBs, the Std-OIT depletion rates of 0.84, 1.2, and 1.48 month^{-1} were obtained for LxV20 ($Std\text{-}OIT_o$ = 200 minutes), BzV20 ($Std\text{-}OIT_o$ =120 minutes), and MzV20 ($Std\text{-}OIT_o$ = 130 minutes), respectively (Figure 6b and Table 3). Hence, LxV20 had both a relatively high $Std\text{-}OIT_o$ value and the slowest depletion rate to reach full depletion after 4.4 months compared to 2.3 months for BzV20, and 2.1 months for MzV20. Thus, for both the 1.5 and 2.0 mm GMBs, the LLDPE GMBs had a longer antioxidant depletion time than the HDPE GMBs due to the higher resistance of their antioxidant package to depletion in chlorinated water.

For the HP-OIT, LxE15 ($HP\text{-}OIT_o$= 890 minutes) depleted to a residual value of 160 minutes (normalized 0.18) after 5.8 months while MxC15 ($HP\text{-}OIT_o$= 960 minutes) depleted to higher residual value of 510 minutes (normalized 0.53) but after 6.6 months (Figure S2a and Table 4). For the 2.0 mm GMBs, the depletion rate of MzV20 ($HP\text{-}OIT_o$= 4600 minutes) was the fastest, giving the shortest depletion time to residual (OIT_r = 2400 minutes, normalized 0.53) of 4.8 months, followed by BzV20 ($HP\text{-}OIT_o$= 3700 minutes) at 7.8 months to residual (OIT_r = 2200 minutes, normalized 0.61) and finally LxV20 ($HP\text{-}OIT_o$= 4600 minutes) took 11.8 months to reach residual (OIT_r = 890 minutes, normalized 0.22; Figure S2b and Table 4).

The results for HP-OIT did not indicate a relationship between the HP-OIT depletion time and the density of the polymer's resin. For instance, the HP-OIT depletion time of the 1.5 mm HDPE GMB was

longer than that for the LLDPE GMB. The opposite was observed for the 2.0 mm GMBs where the HP-OIT depletion time of the LLDPE was the longest, followed by the BPO, and the shortest was the HDPE GMB. These results conform to the conclusion obtained from the Std-OIT depletion results that the antioxidant depletion time is more influenced by the characteristics of the antioxidant package than the polymer structure. However, there is an apparent relationship between the polymer resin's density and the normalized HP-OIT residual values. For both the 1.5 and 2.0 mm GMBs, the normalized HP-OIT residual values for the LLDPE GMBs were less than the HDPE GMBs indicating that less HP-OIT antioxidant/stabilizer package (e.g. HALS) was trapped inside the core of the less crystalline LLDPE compared to the BPO and HDPE GMBs where a GMB with larger amorphous zone may have allowed easier diffusion of antioxidants/stabilizers out to the surface.

GMBs with less crystallinity were affected by more severe chain scission oxidation reactions as implied by the higher normalized MFI values achieved by the less crystalline GMBs examined (Figure 7). For instance, the normalized HLMI for the LLDPE GMBs at 35 months was 1.91 for LxE15, and 4.23 for LxV20 compared to 2.13 for the BPO GMB (BzV20), 1.14 and 1.30 for the HDPE GMBs MxC15 and MzV20, respectively. However, less degradation in Stage A was observed for the LLDPE GMBs compared to the HDPE GMBs (Figure 8) as implied by the normalized values of $F_{b\text{-}SO}$ and $\varepsilon_{b\text{-}SO}$. For the 1.5 mm GMBs, the normalized values of $F_{b\text{-}SO}$ and $\varepsilon_{b\text{-}SO}$ were 0.83 and 0.88 for LxE15 compared to 0.70 and 0.66 for MxC15 (Table 2), while for the 2.0 mm GMBs, the normalized values of $F_{b\text{-}SO}$ and $\varepsilon_{b\text{-}SO}$ were 0.84 and 0.90 for LxV20, 0.84 and 0.89 for BzV20, and 0.66 and 0.73 for MzV20 (Table 2).

Although chain scission oxidation reactions were observed for the LLDPE GMBs examined herein, as implied by the significant increase in the MFI index, the degradation in tensile properties was relatively limited suggesting an oxidation of interlamellar connections (e.g., tie molecules, cilia, and loose loops) which caused a reduction of SCR of LxV20 from an initial value of 25000 hours to 2600 hours corresponding to a normalized value of 10% after 26 months of immersion. The defects in the interlamellar connections associated with oxidative degradation could be more apparent at the slow rate loading of the

notched constant tensile load test compared to the relatively fast loading rate (50 mm/minute) in the tensile test. This could be because there is more time available in the SCR test that decreases the strain hardening of the fibrils and hence decreases the tearing resistance of the polymer (Barry and Delatycki 1992).

To further examine the surface degradation and its effect on the tensile properties, an environmental scanning electron microscope (ESEM; model: FEI-MLA Quanta 650 FEG) was used to monitor the surface condition and development of surface cracks during ageing for HDPE and LLDPE GMBs (MyF3-15 and LxE15). For MyF3-15, majorly disconnected cracks were formed near the surface of the GMB after 6 months ($\varepsilon_{b\text{-}SO}/\varepsilon_{bo}$ = 0.90) of immersion (before the full depletion of HP-OIT), then at 22 months ($\varepsilon_{b\text{-}SO}/\varepsilon_{bo}$= 0.06) a network of cracks extended from both surfaces of the GMB towards its core (Figure 9a). For the GMB LxE15 (Figure 9b), limited surface cracks could be observed at both 6 and 22 months ($\varepsilon_{b\text{-}SO}/\varepsilon_{bo}$= 0.88) that resulted in limited reduction in the tensile properties of this GMB compared to MyF3-15 (i.e., more degradation was observed in the HDPE GMB compared to the LLDPE GMB).

4.3 Effect of GMB's thickness

Previous studies indicated that increasing the GMB thickness resulted in longer OIT depletion time (e.g., Rowe and Ewais 2014); and this may be expected to be the case if all other things are equal. However, other things are not always equal and thickness is only one of several factors that affect the antioxidant depletion time. Other important factors include: (i) type of antioxidant package, (ii) incubation fluid, (iii) incubation temperature, and (iv) morphology of polymer structure. Therefore, this section investigates the effect of GMB thickness on the relative longevity of four HDPE GMBs with thicknesses of 1.5, 2.0 and 2.5 mm and two LLDPE GMB with thickness of 1.5 and 2.0 mm designated as Group 4 GMBs with properties given in Table 1d.

The Std-OIT depletion time for the HDPE GMBs, made from nominally the same MDPE polymer resin (M2) were 1.9 months for 1.5 mm-thick MxC15 ($Std\text{-}OIT_o$ = 160 minutes), 2.1 months for 2.0 mm MzV20 ($Std\text{-}OIT_o$ = 130 minutes), and 7.5 months for 3.0 mm MxV30 ($Std\text{-}OIT_o$ = 250 minutes). Thus, similar to previous studies investigating different thickness GMBs (e.g. Rowe et al. 2014) increasing the

thickness of the HDPE GMB resulted in reducing the Std-OIT depletion rate. The Std-OIT depletion times for the LLDPE GMBs were 4.3 months for 1.5mm LxE15 ($Std\text{-}OIT_o$ = 155 minutes) and 4.4 months for 2mm LxV20 ($Std\text{-}OIT_o$ = 200 minutes; Figure 10b and Table 3). Although the initial Std-OIT of the 2 mm LxV20 was greater than that for the 1.5 mm LxE15 by 30%, both GMBs had essentially the same Std-OIT depletion times. This indicates that LxE15 had a more resistant antioxidant package in chlorinated water than that used in LxV20, and that it was sufficiently better to counteract the difference in both initial value and thickness in chlorinated water.

There was no clear relationship between the GMB's thickness and HP-OIT depletion time for the three HDPE GMBs with the same nominal resin but very different antioxidant packages (MxC15, MzV20, and MxV30). The HP-OIT depletion times were 6.6 months for MxC15 ($HP\text{-}OIT_o$ = 960 minutes; $HP\text{-}OIT_r$= 510 minutes; Resin M2), 4.8 months for MzV20 ($HP\text{-}OIT_o$ = 4600 minutes; $HP\text{-}OIT_r$= 2400 minutes; Resin M2), and 5.7 months for MxV30 ($HP\text{-}OIT_o$ = 1480 minutes; $HP\text{-}OIT_o$= 780 minutes; Resin M2) with a normalized residual value of 0.53· $HP\text{-}OIT_o$ for the three GMBs (Figure S3a and Table 4). This implies that the HP-OIT package of MxC15 was the most resistant to depletion amongst the three HDPE GMBs despite being the thinnest GMB. Also, MzV20 had $HP\text{-}OIT_o$ and $HP\text{-}OIT_r$ values that were 3-fold higher than for MxV30, but the depletion time of MxV30 was longer than MzV20 by a factor of 1.2 suggesting that the greater thickness of MxV30 counteracted the higher initial HP-OIT of MzV20. Another factor could be that the HP-OIT antioxidant/stabilizer package in MxV30 was more stable in chlorinated water.

The HP-OIT depletion times of the LLDPE GMBs LxE15 and LxV20 were 5.8 and 11.8 months, respectively, with HP-OIT residual values equal to 160 and 890 minutes and normalized values of 0.18 and 0.22, respectively (Figure S3b and Table 4). The greater HP-OIT depletion time achieved by LxV20 compared to LxE15 may be due to a combination of a significantly better HP-OIT package and/or higher $HP\text{-}OIT_o$ value for LxV20 (4.6-fold that of LxE15) and the thickness of the GMB.

The results of MFI with time for HDPE GMBs did not show a clear relationship between the GMB thickness and the onset time of oxidation reactions where changes in the MFI were detected after 1 month

for both MxC15 and MxV30, and after 10 months for MzV20. The degradation of tensile properties for the three HDPE GMBs was in Stage A and indicated less decrease in break strain for GMBs with greater thickness. For instance, the normalized $\varepsilon_{b\text{-}SO}$ was 0.66, 0.73, and 0.87 for MxC15, MzV20, and MxV30, respectively (Figure 11a and Table 2). For the LLDPE GMBs, the tensile break strain of both LxE15 and LxV20 decreased to $\varepsilon_{b\text{-}so}$ of about 738% corresponding to normalized values of 0.88 and 0.90, respectively (Figure 11b and Table 2) and the normalized $F_{b\text{-}SO}$ of both GMBs was 0.84 while the absolute $F_{b\text{-}SO}$ was 47 and 66.4 kN/m for LxE15 and LxV20, respectively, indicating that LxV20 still has higher tensile break strength. Thus, based on these results for both HDPE and LLDPE GMBs, using a thicker GMB is better to overcome the anticipated short-term loss of tensile strength that occurs due to surface oxidation by chlorine species in Stage A, because a GMB with greater thickness will have a thicker non-oxidized core.

The above results showed that antioxidant depletion rate for GMBs exposed to chlorinated water is controlled by two major mechanisms: chemical attack by chlorine species responsible for antioxidant depletion, and outward diffusion of antioxidants (Hassinen et al. 2004). The type, molecular structure, relative antioxidants/monomer size, and molecular weight of the antioxidant package are factors that affect the diffusion of the antioxidants (Roe et al. 1974; Möller and Gevert 1994; Hsuan and Koerner 1998, Rimal and Rowe 2009) and in subsequent affecting the percentage of antioxidants consumed by either mechanism (Hassinen et al. 2004). This could explain why a GMB with 1.5 mm thickness (MyF3-15) had longer antioxidant depletion time than a 2.0 mm-thick GMB (MzV20). These GMBs were produced by two different manufacturers with different resins and different antioxidant package. Thus, the combination of resin/antioxidant package had greater influence on antioxidant depletion time compared to GMB thickness in this case.

5 Discussion of Longevity of GMBs in Chlorinated Water

The degradation of GMBs stabilized with HALS, when immersed in chlorinated water, as reported by Abdelaal and Rowe (2019), Abdelaal et al. (2019), and the current paper, can be explained as summarized below. Sodium hypochlorite disassociates in water into, primarily, two species: (i) hypochlorous acid

(HOCl$^-$), and (ii) hypochlorite (ClO$^-$) where hypochlorite ion (ClO$^-$) is the main oxidizing agent in chlorinated water whose pH is greater than 8 (Montes et al. 2012) as is the case in the current study (pH = 9.9). Chlorine species extract hydrogen atoms from the polymer, followed by diffusion of oxygen from the chlorine species into the polymer forming carbonyl groups on the GMB's surface (Whelton et al. 2011; Montes et al. 2012; Mitroka et al. 2013; Yu et al. 2013) that increase the hydrophilicity of GMB's surface (Whelton et al. 2011) and results in oxidation of the GMB's surface before the full depletion of antioxidants (Figures 2a-2k). Shortly after incubation in chlorinated water, the surface oxidation causes the formation of disconnected surface cracks that reduce the tensile break properties and SCR (Abdelaal et al. 2019) to values designated as $F_{b\text{-}SO}$, $\varepsilon_{b\text{-}SO}$, and SCR_{SO} in Stage A. The length of Stage A is hypothesized to be affected by the extent of precipitation of sodium hypochlorite by-products on the GMB surface that tend to protect the GMB's core (Abdelaal and Rowe, 2019) and the presence of the immobile residual HALS in the amorphous zone in the GMB core that may impede the interaction of chlorine species with the GMB core, and hence the onset of Stage B (Abdelaal et al. 2019) as implied from the comparison between LxE15 ($HP\text{-}OIT_o$= 890 minutes; stabilized with HALS; Resin L1) and LxD15 ($HP\text{-}OIT_o$= 350 minutes; with a trace of HALS; resin L1). But, the primary factor that appeared to affect the length of Stage A and the subsequent degradation in Stage B is the resistance of the polymer resin to crack formation and further connectivity of these cracks that extend gradually from the GMB surface towards its core, then turn into a connected network of cracks during ageing resulting at a certain point in a faster degradation rate (Stage B) of tensile properties and SCR until severe degradation is reached (t_{sd}). This was verified by the better performance of LxE15 with a lower HP-OIT residual value ($HP\text{-}OIT_r$= 160 minutes; resin L1) compared to MyF3-15 with a higher ($HP\text{-}OIT_r$= 500 minutes; resin M6) as implied from the ESEM photos (Figure 9).

6 Conclusions

The performance of twelve GMBs was examined when immersed chlorinated water (0.5 ppm simulant) at 85^{o}C and the effect of various factors on the longevity of the GMBs including resin type, initial OIT, GMB

542 density, and thickness, were investigated. For the GMBs and test conditions (e.g., temperature and chlorine
543 concentration) investigated, the following conclusions were reached:

544 1- The degradation trend of the HALS stabilized GMBs examined was consistent with that reported
545 by Abdelaal et al. (2019) wherein the GMB experienced degradation shortly after immersion until
546 it stabilized at a value (e.g., a normalized break strain $0.48 \leq \varepsilon_{b\text{-}SO}/\varepsilon_{bo} \leq 0.90$) for a lag period (Stage
547 A) followed by a second stage of degradation (Stage B) until severe degradation was reached at a
548 time t_{sd}.
549 2- The choice of resin played an important role in resisting the degradation by chlorinated water
550 (evidenced from the different t_{sd} of GMBs produced by different resin manufacturers), with some
551 resins far outperforming others. However, the results also suggest that HALS played a role in
552 delaying the GMB degradation in chlorinated water as was evident from the better resistance to
553 degradation of LxE15 (with HALS) compared to LxD15 (traces of HALS) although they were
554 produced from nominally the same resin.
555 3- The resistance of antioxidant/stabilizer package to an incubation fluid greatly affected the depletion
556 rate with the results showing that a "good" package could give better performance for a thinner or
557 lower density resin than might be achieved with a thicker HDPE with an inferior
558 antioxidant/stabilizer package. This was evident from the longer Std-OIT depletion times of some
559 LLDPE GMBs than for HDPE GMBs of similar thickness and by the longer Std-OIT depletion
560 times of some 1.5 mm GMBs than 2.0 mm-thick GMBs.
561 4- Higher initial Std-OIT and HP-OIT did not necessarily result in longer time to severe degradation
562 (t_{sd}). For example, MyF3-15 with modestly high initial OIT values reached severe degradation
563 before other GMBs with lower initial Std-OIT and/or HP-OIT.
564 5- Less degradation of tensile properties in Stage A did not result in longer time to severe degradation,
565 t_{sd}. For instance, MyF3-15 had the highest normalized $\varepsilon_{b\text{-}SO}$ value amongst the GMBs tested but had
566 the lowest t_{sd} of all GMBs examined except for MyEW15.

6- MFI test results suggest that the chain scission reactions in LLDPE GMBs were more severe compared to HDPE GMBs.

In short, the relative performance of a GMB in chlorinated water cannot be predicted based on the initial Std-OIT, HP-OIT, resin, or thickness. The performance depends on both the choice of the resin and the antioxidant package and can really only be assessed by accelerated immersion testing similar to that described herein.

7 Acknowledgements

The research reported in this paper was supported by the Natural Sciences and Engineering Research Council of Canada (NSERC) grant (A1007) to Dr. R.K. Rowe. The equipment used was funded by Canada Foundation for Innovation (CFI) and the Government of Ontario's Ministry of Research and Innovation.

8 References

Abdelaal, F.B., and Rowe, R.K. 2014. Effect of chlorinated water on the antioxidant depletion of HDPE geomembrane without HALS. *In* Proceedings of the 10th International Conference on Geosynthetics, Berlin.

Abdelaal, F.B and Rowe, R.K. 2017. Effect of high pH found in low-level radioactive waste leachates on the antioxidant depletion of a HDPE geomembrane, Journal of Hazardous, Toxic, and Radioactive Waste, **21**(1); 10.1061/(ASCE)HZ.2153-5515.0000262, D4015001

Abdelaal, F.B., and Rowe, R.K. 2019. Degradation of a HDPE geomembrane without HALS in chlorinated water. Geosynthetics International, https://doi.org/10.1680/jgein.19.00016.

Abdelaal, F.B., Rowe, R.K., Smith, M., Brachman, R.W.I., and Thiel, R. 2012. Antioxidant depletion from HDPE and LLDPE geomembranes without HALS in extremely low pH solution. *In* The 2nd Pan American Geosynthetic Conference and Exhibition, GeoAmericas 2012.

Abdelaal, F.B., Rowe, R.K. and Islam, M.Z. 2014. Effect of leachate composition on the long-term performance of a HDPE geomembrane, Geotextiles and Geomembranes, **42**(4):348-362.

Abdelaal, F. B., Morsy, M.S., and Rowe, R.K. 2019. Long-term performance of a HDPE geomembrane stabilized with HALS in chlorinated water. Geotextiles and Geomembranes, **47**(6), 815-830.

ASTM 2004. "Standard test method for determining tensile properties of non-reinforced polyethylene and nonreinforced flexible polypropylene geomembranes". American Society for Testing and Materials D6693, West Conshohocken, PA.

ASTM 2006. "Standard test method for oxidative induction time of polyolefin geosynthetics by high pressure differential scanning calorimetry". American Society for Testing and Materials D5885, West Conshohocken, PA.

ASTM 2007. "Standard test method for oxidative induction time of polyolefins by differential scanning calorimetry". American Society for Testing and Materials D3895, West Conshohocken, PA.

ASTM 2010. "Standard test method for density of plastics by the density-gradient technique". American Society for Testing and Materials D1505, West Conshohocken, PA.

ASTM 2012. "Standard method for measuring the nominal thickness of geosynthetics". American Society for Testing and Materials D5199, West Conshohocken, PA.

ASTM 2013. "Standard test method for melt flow rates of thermoplastics by extrusion plastometer". American Society for Testing and Materials D1238, West Conshohocken, PA.

ASTM 2018, "Standard test method for melting and crystallisation temperatures by thermal analysis". American Society for Testing and Materials E794, West Conshohocken, PA.

ASTM 2019. "Standard test method for evaluation of stress crack resistance of polyolefin geomembranes using notched constant tensile load test". American Society for Testing and Materials D5397, West Conshohocken, PA.

Awad, R., Morsy, M.S., and Rowe, R.K. 2018. The evolution of melt thermograms of HDPE, LLDPE and blended geomembranes incubated at 105°C. *In* proceedings of 11ICG , Seoul, South Korea, CD-ROM, 8p.

Barry, D. B., and Delatycki, O. (1992). The effect of molecular structure and polymer morphology on the fracture resistance of high-density polyethylene. Polymer, **33**(6): 1261-1265.

Eldesouky, H.M.G. Brachman, R.W.I 2018. Calculating local geomembrane strains from a single gravel particle with thin plate theory. Geotextiles and Geomembranes, **46**(1): 101-110.

Eng, J., Sassi, T., Steele, T., and Vitarelli, G. 2011. The Effects of Chlorinated Water on Polyethylene Pipes. Plastics Engineering, **67**(9): 18.

Eun, J., Tinjum, J., Benson, C., and Edil, T. 2014. Volatile Organic Compound (VOC) Transport through a Composite Liner with Co-Extruded Geomembrane Containing Ethylene Vinyl-Alcohol (EVOH). Geo-Congress 2014 Technical Papers: pp. 1960-1969.

Ewais, A.M.R., and Rowe, R.K. (2014). Effect of aging on the stress crack resistance of an HDPE geomembrane. Polymer degradation and stability, **109**: 194-208.

627 Ewais, A.M.R., Rowe, R.K., Rimal, S. and Sangam, H.P. 2018. 17-year elevated temperature study of
628 HDPE geomembrane longevity in air, water and leachate, Geosynthetics International, **25**(5): 525-
629 544.
630 Fair, G. M., Morris, J.C., Lu Chang, S., Weil, I., and Burden, R.P. 1948. The behavior of chlorine as a water
631 disinfectant. Journal (American Water Works Association), **40**(10): 1051-1061.
632 GRI-GM13 2016. Standard specification for test methods, test properties and testing frequency for high
633 density polyethylene (HDPE) smooth and textured Geomembranes: GRI Test Method
634 Geomembrane 13, Revision 14: January 6, 2016, *Geosynthetic Research Institute*, Folsom, Pa.
635 Hassinen, J., Lundbäck, M., Ifwarson, M., and Gedde, U.W. 2004. Deterioration of polyethylene pipes
636 exposed to chlorinated water. Polymer Degradation and Stability, **84**(2): 261-267.
637 Hsuan, Y.G., and Koerner, R.M. 1998. Antioxidant depletion lifetime in high density polyethylene
638 geomembranes. Journal of Geotechnical and Geoenvironmental Engineering, **124**(6): 532-541.
639 Joo, J.C., Kim, J.Y., and Nam, K. (2004) "Mass transfer of organic compounds in dilute aqueous solutions
640 into high density polyethylene geomembrane" Journal of Environmental Engineering **130**(2): 175-
641 183.
642 Jones, D.D. and Rowe, R.K. 2016. BTEX migration through various geomembranes and vapour barriers.
643 ASCE Journal of Geotechnical and Geoenvironmental Engineering, **142**(10):04016044-1 to 12,
644 DOI: 10.1061/(ASCE)GT
645 Kim, B. R., Anderson, J. E., Mueller, S. A., Gaines, W. A., and Kendall, A. M. 2002. Literature review-
646 efficacy of various disinfectants against Legionella in water systems. Water Research, **36**(18):
647 4433-4444.
648 Lundbäck, M. 2005. Long term performance of polyolefins in different environments including chlorinated
649 water: antioxidant consumption and migration and polymer degradation (Doctoral dissertation,
650 KTH).
651 McWatters, R. and Rowe, R.K. 2009. Transport of volatile organic compounds through PVC and LLDPE
652 geomembranes from both aqueous and vapour phases. Geosynthetics International, **16**(6): 468-481.
653 McWatters, R. and Rowe, R.K. 2010. Diffusive transport of VOCs through LLDPE and two Co-Extruded
654 Geomembranes. ASCE Journal of Geotechnical and Geoenvironmental Engineering, **136**(9): 1167-
655 1177.
656 McWatters, R.S. and Rowe, R.K. 2015. Permeation of volatile organic compounds through EVOH thin-
657 film membranes and co-extruded LLDPE/EVOH/LLDPE geomembrane. ASCE Journal of
658 Geotechnical and Geoenvironmental Engineering, **141**(2), 0401409: 1-15.

659 Mendes, M., Touze-Foltz, N., Gardoni, M. dG., Ahari, M., and Mazéas, L. 2013. Quantification of diffusion
660 of phenolic compounds in virgin GCL and in GCL after contact with a synthetic leachate.
661 Geotextiles and Geomembranes **38**: 16-25
662 Mills, A. 2011. The Effects of Chlorine on Very Low Density Thermoplastic Olefins. *In* Geo-Frontiers
663 2011: Advances in Geotechnical Engineering (pp. 2173-2182).
664 Mitroka, S. M., Smiley, T. D., Tanko, J. M., and Dietrich, A. M. 2013. Reaction mechanism for oxidation
665 and degradation of high density polyethylene in chlorinated water. Polymer degradation and
666 stability, **98**(7): 1369-1377.
667 Möller, K., and Gevert, T. 1994. An FTIR solid-state analysis of the diffusion of hindered phenols in
668 low-density polyethylene (LDPE): The effect of molecular size on the diffusion
669 coefficient. Journal of applied polymer science, **51**(5): 895-903.
670 Montes, J. C., Cadoux, D., Creus, J., Touzain, S., Gaudichet-Maurin, E., and Correc, O. 2012. Ageing of
671 polyethylene at raised temperature in contact with chlorinated sanitary hot water. Part I–Chemical
672 aspects. Polymer degradation and stability, **97**(2): 149-157.
673 Morsy, M.S., and Rowe, R.K. 2017a. Effect of texturing on antioxidant depletion rate from HDPE
674 geomembranes. *In* Proceedings of the 19th International Conference on Soil Mechanics and
675 Geotechnical Engineering (pp. 3175-3178), Seoul, South Korea.
676 https://www.issmge.org/uploads/publications/1/45/06-technical-committee-21-tc215-22.pdf
677 Morsy, M.S., and Rowe, R.K. 2017b. Performance of blended polyolefin geomembrane in various
678 incubation media based on Std-OIT. *In* Geotechnical Frontiers 2017 (pp. 1-10).
679 https://ascelibrary.org/doi/abs/10.1061/9780784480434.001
680 Morsy, M.S., and Rowe, R.K. 2020. Effect of texturing on the longevity of high-density polyethylene
681 (HDPE) geomembranes in municipal solid waste landfills. Canadian Geotechnical Journal, **57**(1):
682 61-72.
683 Morsy, M.S., Rowe, R.K., and Abdelaal, F.B. 2016. Antioxidant depletion from HDPE and LLDPE
684 geomembranes in chlorinated water. *In* proceedings of 3rd Pan-American Conference on
685 Geosynthetics (pp. 76-81), Florida, USA.
686 Morsy, M.S., Abdelaal, F.B., and Rowe, R.K. 2019. Performance of blended polyolefin and LLDPE
687 geomembranes in heap leach pads based on OIT. *In* proceedings of Geosynthetics conference 2019
688 (pp. 174-182), Texas, USA.
689 Rimal, S., and Rowe, R.K. 2009. Diffusion modelling of OIT depletion from HDPE geomembrane in
690 landfill applications. Geosynthetics International, **16**(3): 183-196.
691 Roe, R. J., Bair, H.E., and Gieniewski, C. 1974. Solubility and diffusion coefficient of antioxidants in
692 polyethylene. Journal of Applied Polymer Science, **18**(3): 843-856.

693 Rowe, R.K. 1988. Contaminant migration through groundwater: The role of modelling in the design of
694 barriers. Canadian Geotechnical Journal, **25**(4):778-798.
695 Rowe, R.K. 1998. Geosynthetics and the minimization of contaminant migration through barrier systems
696 beneath solid waste. Keynote paper, Proceedings of the 6th International Conference on
697 Geosynthetics, Atlanta, March, 1, pp. 27-103.
698 Rowe, R.K. 2005. Long-term performance of contaminant barrier systems, 45th Rankine Lecture.
699 Geotechnique, **55**(9):631-678.
700 Rowe, R.K 2012. Short and long-term leakage through composite liners, The 7th Arthur Casagrande
701 Lecture. Canadian Geotechnical Journal, **49**(2): 141-169.
702 Rowe, R.K. 2018, Environmental geotechnics: looking back, looking forward (16th Croce Lecture).
703 Italian Geotechnical Journal. **4**:8-40, dx.doi.org/10.19199/2018.4.0557-1405.008.
704 Rowe, R.K. 2020. Protecting the environment with geosynthetics - The 53rd Karl Terzaghi Lecture.
705 ASCE Journal of Geotechnical and Geoenvironmental Engineering, (in press).
706 Rowe, R.K. and Abdelaal, F.B. 2016. Antioxidant depletion in HDPE Geomembrane with HALS in low
707 pH heap leach environment. Canadian Geotechnical Journal, **53**(10):1612-1627, ,
708 Rowe, R.K. and Arnepalli, D.N. 2008. "The effects of landfill temperature on the contaminant transport
709 through a composite liner", 12th International Conference of International Association for Computer
710 Methods and Advances in Geomechanics (IACMAG), Goa, India, pp. 2398-2404.
711 Rowe, R.K. and Booker, J.R. 1995. A finite layer technique for modelling complex landfill history,
712 Canadian Geotechnical Journal, **32**(4):660-676.
713 Rowe, R. K., and Ewais, A. M. R. 2014. Antioxidant depletion from five geomembranes of same resin but
714 of different thicknesses immersed in leachate. Geotextiles and Geomembranes, **42**(5): 540-554.
715 Rowe, R.K. and Ewais, A.R. 2015. Ageing of exposed geomembranes at locations with different
716 climatological conditions. Canadian Geotechnical Journal, **52** (3):326-343.
717 Rowe, R.K. and Hoor, A. 2009. Predicted temperatures and service lives of secondary geomembrane
718 landfill liners. Geosynthetics International, **16**(2):71-82.
719 Rowe, R.K. and Islam, M.Z. 2009. Impact on landfill liner time-temperature history on the service-life of
720 HDPE geomembranes. Waste Management, **29**: 2689-2699.
721 Rowe, R.K., and Sangam, H.P. 2002. Durability of HDPE geomembranes. Geotextiles and
722 Geomembranes, **20**(2): 77-95.
723 Rowe, R.K and Yu, Y. 2019. Magnitude and significance of tensile strains in geomembrane landfill liners.
724 Geotextiles and Geomembranes, **47**(3):429-458.
725 Rowe, R.K. Sangam, H.P. and Lake, C.B 2003. Evaluation of an HDPE geomembrane after 14 years as a
726 leachate lagoon liner. Canadian Geotechnical Journal, **40**(3):536-550**.**

727 Rowe, R. K., Quigley, R. M., Brachman, R.W.I., and Booker, J. R. 2004. Barrier systems for waste disposal
728 facilities (No. Ed. 2). Spon Press.
729 Rowe, R.K., Islam, M.Z. and Hsuan, Y.G. 2008. Leachate chemical composition effects on OIT depletion
730 in HDPE geomembranes. Geosynthetics International. **15**(2):136-151
731 Rowe, R. K., Rimal, S., and Sangam, H. 2009. Ageing of HDPE geomembrane exposed to air, water and
732 leachate at different temperatures. Geotextiles and Geomembranes. **27**(2): 137-151.
733 Rowe, R.K., Chappel, M.J., Brachman, R.W.I. and Take, W.A. 2012a. Field monitoring of geomembrane
734 wrinkles at a composite liner test site. Canadian Geotechnical Journal. **49**(10): 1196-1211
735 Rowe, R.K., Yang, P., Chappel, M.J., Brachman, R.W.I. and Take, W.A. 2012b. Wrinkling of a
736 geomembrane on a compacted clay liner on a slope, Invited paper for Special Issue on
737 Geosynthetics, Geotechnical Engineering. Journal of the South East Asian Geotechnical Society,
738 **43**(3): 11-18.
739 Rowe, R.K., Jones, D.D., and Rutter, A. 2016a. Polychlorinated biphenyl diffusion through HDPE
740 geomembrane. Geosynthetics International, **23**(6):408-421.
741 Rowe, R.K., Saheli, P.T., and Rutter, A. 2016b. Partitioning and diffusion of PBDEs through an HDPE
742 geomembrane. Waste Management, **55** 191–203.
743 Rowe, R.K., Abdelaal, F.B., Zafari, M., Morsy, M.S., and Priyanto, D. 2019a. An approach to HDPE
744 geomembrane selection for challenging design requirements. Canadian Geotechnical Journal,
745 https://doi.org/10.1139/cgj-2019-0572.
746 Rowe, R.K., Morsy, M.S., and Ewais, A.M.R. 2019b. Representative stress crack resistance of polyolefin
747 geomembranes used in waste management. Waste Management, **100**: 18-27.
748 Saheli, P.T. and Rowe, R.K. 2016a. Diffusive Transport of Bisphenol-A (BPA) through a Geosynthetic
749 Clay Liner (GCL). Geotextiles and Geomembranes, **44**(5):731-738,
750 Saheli, P.T., Rowe, R.K. and Rutter, A. 2016b. Diffusion of bisphenol-A (BPA) through an HDPE
751 geomembrane. Geosynthetics International, **23**(6):452-462,
752 Sangam, H.P. and Rowe, R.K 2001. Migration of dilute aqueous organic pollutants through HDPE
753 geomembranes. Geotextiles and Geomembranes, **19**(6):329-357.
754 Sangam, H.P. and Rowe, R.K 2002. Effects of exposure conditions on the depletion of antioxidants from
755 HDPE geomembranes. Canadian Geotechnical Journal, **39**(6):1221-1230.
756 Sangam, H.P. and Rowe, R.K 2005. Effect of surface fluorination on diffusion through an HDPE
757 geomembrane. ASCE Journal of Geotechnical and Geoenvironmental Engineering, **131**(6):694-
758 704.
759 Scheirs, J. 2009. A guide to polymeric geomembranes: a practical approach. John Wiley and Sons.

760 Take, W.A., Chappel, M.J., Brachman, R.W.I. and Rowe, R.K. 2007. Quantifying geomembrane wrinkles
761 using aerial photography and digital image processing, Geosynthetics International, **14**(4) 219-227.
762 Take, W.A, Watson, E., Brachman, R.W.I., and Rowe, R.K. 2012. Thermal expansion and contraction of
763 geomembrane liners subjected to solar exposure and backfilling. ASCE Journal of Geotechnical
764 and Geoenvironmental Engineering, **138**(11): 1387 – 1397.
765 Take W.A., Rowe, R.K, Brachman, R.W.I., and Arnepalli, D.N. 2015. Thermal exposure conditions for a
766 composite liner with a black geomembrane exposed to solar radiation, Geosynthetics International,
767 **22**(1): 93-109.
768 Tian, K., Benson, C.H., Tinjum, J.M., and Edil, T.B. 2017. Antioxidant depletion and service-life prediction
769 for HDPE geomembranes exposed to low-level radioactive waste leachate, ASCE JGGE,
770 **143**(6):04017011, https://doi.org/10.1061/(ASCE)GT.1943-5606.0001643
771 Tian, K., Benson,C.H. Yang,Y-M and Tinjum, J.M. 2018. Radiation dose and antioxidant depletion in a
772 HDPE geomembrane. Geotextiles and Geomembranes, **46**(4): 426-435.
773 Tognon, A.R. Rowe, R.K. and Moore, I.D. 2000. Geomembrane strain observed in large-scale testing of
774 protection layers. ASCE Journal of Geotechnical and Geoenvironmental Engineering,
775 126(12):1194-1208.
776 Touze-Foltz, N. Rowe, R.K. and D'equennoi, C. 1999. Liquid flow through composite liners due to
777 geomembrane defects: Analytical solutions for axisymmetric and two-dimensional problems.
778 Geosynthetics International, **6**(6):455-479.
779 Whelton, A. J., Dietrich, A. M., and Gallagher, D. L. 2011. Impact of chlorinated water exposure on
780 contaminant transport and surface and bulk properties of high-density polyethylene and cross-
781 linked polyethylene potable water pipes. Journal of Environmental Engineering, **137**(7): 559-568.
782 Yoshida, H. and Rowe, R.K. 2003. Consideration of landfill liner temperature, *In* Proceedings of 8th
783 International Waste Management and Landfill Symposium, S. Margherita di Pula, Cagliari,
784 Sardinia, Italy, October, CD-ROM, 9p.
785 Yu, W., Azhdar, B., Andersson, D., Reitberger, T., Hassinen, J., Hjertberg, T., and Gedde, U. W. 2011.
786 Deterioration of polyethylene pipes exposed to water containing chlorine dioxide. Polymer
787 degradation and stability, **96**(5): 790-797.
788 Yu, W., Sedghi, E., Nawaz, S., Hjertberg, T., Oderkerk, J., Costa, F. R., and Gedde, U. W. 2013.
789 Assessing the long-term performance of polyethylene stabilised with phenolic antioxidants
790 exposed to water containing chlorine dioxide. Polymer testing, **32**(2): 359-365.
791

List of Figures:

Figure 1. Variation of different index properties in chlorinated water (0.5 ppm free chlorine) at 85°C for: (a) MxA15 (without HALS; Abdelaal and Rowe 2019) & (b) MxC15 (with HALS; Abdelaal et al. 2019). t_{sd} = time to severe degradation and t_{NF} = time to nominal failure.

Figure 2. Degradation trends of 12 GMBs in chlorinated water (0.5 ppm free chlorine): (a) MyF1-15; (b) MyF2-15; (c) LxE15; (d) LxV20; (e) BzV20; (f) MxV30; (g) MxC15; (h) MzV20; (i) MyEW15; (j) MyF3-15; (k) MyE15; (l) LxD15.

Figure 3. The effect of initial Std-OIT value on depletion time of 1.5 mm GMBs immersed in Chlorinated water (0.5 ppm free chlorine) at 85°C: (a) HDPE GMBs; (b) LLDPE GMBs.

Figure 4. The effect of initial OIT value on MFI of 1.5 mm GMBs immersed in Chlorinated water (0.5 ppm free chlorine) at 85°C: (a) HDPE; (b) LLDPE. Error bars represent range of results. Last data point for MyE15 & MyF3-15 was 22 months because there was no enough GMB material for tensile & MFI tests at the time interval of 22-35 months.

Figure 5. The effect of initial OIT value on degradation of tensile break strain with incubation time for 1.5 mm GMBs immersed in Chlorinated water (0.5 ppm free chlorine) at 85°C: (a) HDPE; (b) LLDPE. Error bars represent range of results. Last data point for MyE15 & MyF3-15 was 22 months because there was no enough GMB material for tensile & MFI tests at the time interval of 22-35 months.

Figure 6. Variation of Std-OIT with incubation time in chlorinated water (0.5 ppm free chlorine) at 85°C for different GMB resin types: (a) 1.5 mm thick HDPE (MxC15) and LLDPE GMB (LxE15); (b) 2.0 mm thick HDPE (MzV20), LLDPE (LxV20), and BPO (BzV20) GMBs. The arrow indicates the antioxidant depletion time.

-**Figure 7.** Comparison between changes in HLMI with incubation time for LLDPE, BPO, and HDPE GMBs immersed in Chlorinated water (0.5 ppm free chlorine) at 85°C: (a) 1.5 mm thick HDPE (MxC15) and LLDPE GMB (LxE15); and (b) 2.0 mm thick HDPE (MzV20), LLDPE (LxV20), and BPO (BzV20) GMBs.

Figure 8. Comparison between degradation of physical properties with incubation time for LLDPE, BPO, and HDPE GMBs immersed in Chlorinated water (0.5 ppm free chlorine) at 85°C: (a) 1.5 mm thick HDPE (MxC15) and LLDPE GMB (LxE15); and (b) 2.0 mm thick HDPE (MzV20), LLDPE (LxV20), and BPO (BzV20) GMBs.

Figure 9. ESEM photos for GMBs incubated in chlorinated water (0.5 ppm free chlorine) at 85°C at different aging times of 0, 6, and 22 months: (a) MyF3-15, and (b) LxE15.

826 **Figure 10.** Variation of Std-OIT depletion with incubation time for GMBs of different thickness immersed
827 in Chlorinated water (0.5 ppm free chlorine) at 85°C: (a) HDPE GMBs; and (b) LLDPE GMBs.
828 The arrow indicates the antioxidant depletion time.
829 **Figure 11.** Variation of tensile break strain with incubation time for GMBs of different thickness
830 immersed in Chlorinated water (0.5 ppm free chlorine) at 85°C: (a) HDPE GMBs; and (b)
831 LLDPE GMBs.

832 ## List of Tables:

833 **Table 1.a.** Initial properties of GMBs- Group 1.
834 **Table 1.b.** Initial properties of GMBs- Group 2.
835 **Table 1.c.** Initial properties of GMBs- Group 3.
836 **Table 1.d.** Initial properties of GMBs- Group 4.
837 **Table 2.** Antioxidant depletion time, degradation of tensile properties in Stage (A), and time to
838 brittleness of the 12 GMBs immersed in chlorinated water (0.5 ppm free chlorine) at 85°C;
839 rounded to 2 significant digits.
840 **Table 3.** Summary of Std-OIT results for 12 GMBs immersed in chlorinated water (0.5 ppm free
841 chlorine) at 85°C.
842 **Table 4.** Summary of HP-OIT results for 12 GMBs immersed in chlorinated water (0.5 ppm free
843 chlorine) at 85°C.
844

845 ## Supplementary material:

846 **Figure S1.** The effect of initial HP-OIT value on depletion time of 1.5 mm GMBs immersed in
847 Chlorinated water (0.5 ppm free chlorine) at 85°C: (a) HDPE GMBs; (b) LLDPE GMBs. Error bars
848 represent range of results.
849 **Figure S2.** Variation of Std-OIT with incubation time in chlorinated water (0.5 ppm free chlorine) at 85°C
850 for different GMB resin types: (a) 1.5 mm thick HDPE (MxC15) and LLDPE GMB (LxE15); and (b) 2.0
851 mm thick HDPE (MzV20), LLDPE (LxV20), and BPO (BzV20) GMBs. Error bars represent range of
852 results.
853 **Figure S3.** Variation of HP-OIT depletion with incubation time for GMBs of different thickness immersed
854 in Chlorinated water (0.5 ppm free chlorine) at 85°C: (a) HDPE GMBs; and (b) LLDPE GMBs. Error bars
855 represent range of results.
856

Table 1.a. Initial properties of GMBs- Group 1.

Property	Method	Unit	Mean ± SD[1]				
Designator	--	--	MyE-15	MyEW-15	LxD15	LxE15	MxA15[4]
Type	--	--	HDPE	HDPE	LLDPE	LLDPE	HDPE
Resin type	--	--	M7	M8	L1-1	L1-2	M1
Manufacturing technique	--	--	Blown film	Blown film	Blown film	Blown film	Blown film
Production date	--	--	2012	2012	2011	2011	2005
Nominal thickness	ASTM 2012	mm	1.5	1.5	1.5	1.5	1.5
Resin density [2]	--	g/cm^3	0.938	0.937	0.924	Not supplied	0.937
GMB density [2]	ASTM 2010	g/cm^3	0.945	0.943	Not supplied	Not supplied	0.947
Crystallinity [3]	ASTM 2018	%	51±2.00	47±0.03	38±0.01	36±1.3	41±2.7
Std-OIT	ASTM 2007	min	150±7	170±5	190 ± 5	155 ± 5	115±2
HP-OIT	ASTM 2006	min	1300±90	670±17	350±13	890±25	260±10
HLMI (21.6kg)	ASTM 2013	g/10min	12.3±0.40	14.1±0.70	13.38±0.8	14.7±0.25	15.9±0.30
LLMI (2.16 kg)		g/10min	0.1±0.002	0.132±0.001	0.141±0.003	0.153±0.011	0.11±0.005
Melt flow ratio (MFR)		unitless	120	107	94	90	146
SCR	ASTM 2019	hrs	13000±1300	4500±1300	20000±5500	>18000	720±130
Tensile property	ASTM 2004		Cross machine direction				
Break stress	Type IV	kN/m	55±1.1	60±1.3	55 ± 1.8	53± 3.8	54±3
Break strain		%	920±60	930±50	980± 34	980 ± 92	896±54
Break stress	Type V	kN/m	58±1.7	62±1.7	57±1.7	56±2.5	57±3
Break strain		%	800±40	860±54	840±40	800±28.3	816±9

[1] Standard deviation; [2] Provided by GMB manufacturer; [3] Encapsulated;[4] from Abdelaal and Rowe (2019). GMBs-Group 1 was used to investigate the effect of resin and role of HALS on the performance of GMBs in chlorinated water.

Table 1.b. Initial properties of GMBs- Group 2.

Property	Method	Unit	Mean ± SD[a]					
Designator	--	--	MyF1-15	MyF2-15	MyF3-15	MyE-15	LxD15	LxE15
Type	--	--	HDPE	HDPE	HDPE	HDPE	LLDPE	LLDPE
Resin type	--	--	M4	M5	M6	M7	L1-1	L1-2
Manufacturing technique	--	--	Blown film	Blown film	Flat die	Blown film	Blown film	Blown film
Production date	--	--	2013	2013	2013	2012	2011	2011
Nominal thickness	ASTM 2012	mm	1.5	1.5	1.5	1.5	1.5	1.5
Resin density [b]	--	g/cm^3	0.937	0.936	0.933	0.938	0.924	Not supplied
GMB density [b]	ASTM 2010	g/cm^3	0.945	0.943	0.945	0.945	Not supplied	Not supplied
Crystallinity [c]	ASTM 2018	%	50±1.9	50±3.0	51±1.4	51±2.0	38±0.0	36±1.3
Std-OIT	ASTM 2007	min	160±5	190±3	210±8	150±7	190 ± 5	155 ± 5
HP-OIT	ASTM 2006	min	1100±110	780±62	1300±90	1300±100	350±13	890±25
HLMI (21.6kg)	ASTM 2013	g/10min	11.8±0.30	10.2±0.2	17.3±0.3	12.3±0.40	13.4±0.8	14.7±0.3
LLMI (2.16 kg)		g/10min	0.096±0.001	0.084±0.002	0.74±0.044	0.1±0.002	0.141±0.003	0.153±0.011
Melt flow ratio (MFR)		unitless	120	120	23	120	94	90
SCR	ASTM 2019	hrs	7600±1900	8100±290	6500±2200	13000±1300	20000±5500	>18000
Tensile property	ASTM 2004	Cross machine direction						
Break stress	Type IV	kN/m	62±0.9	60±1.1	59 ±1.5	55±1.1	55 ± 1.8	53 ± 3.8
Break strain		%	990±16	930±16	960±10	920±60	980± 34	980 ± 92
Break stress	Type V	kN/m	60± 2.0	59± 3	56±2	57±1.7	57±1.7	56±2.5
Break strain		%	800±28	744±46	792±18	800±40	840±40	800±28.3

[a] Standard deviation; [b] Provided by GMB manufacturer; [c] Encapsulated. GMBs-Group 2 was used to investigate the effect of initial OIT value on the OIT depletion time and longevity of GMBs in chlorinated water.

Table 1.c. Initial properties of GMBs- Group 3.

Property	Method	Unit	Mean ± SD[a]				
Designator	--	--	MxC15	LxE15	MzV20	BzV20	LxV20
Type	--	--	HDPE	LLDPE	HDPE	Blended	LLDPE
Resin type	--	--	M2-1	L1-2	M2-2	B2	L2
Manufacturing technique	--	--	Blown film	Blown film	Blown film	Blown film	Blown film
Production date	--	--	2008	2011	2014	2014	2014
Nominal thickness	ASTM 2012	mm	1.5	1.5	2.0	2.0	2.0
Resin density [b]	--	g/cm^3	0.936	Not supplied	Not supplied	Not supplied	0.919
GMB density [b]	ASTM 2010	g/cm^3	0.946	Not supplied	>0.941	0.936	0.934
Crystallinity [c]	ASTM 2018	%	56±2	36±1.3	53±2.2	50±1.3	41±0.8
Std-OIT	ASTM 2007	min	160± 2	155 ± 5	130 ± 6	120 ± 6	200± 12
HP-OIT	ASTM 2006	min	960±17	890±25	4600±160	3700 ± 400	4100±70
HLMI (21.6kg)	ASTM 2013	g/10min	13.9±0.8	14.7±0.3	11.9±0.6	14.6±0.6	14.9±0.9
LLMI (2.16 kg)		g/10min	0.12±0.003	0.153±0.011	0.094±0.004	0.22±0.011	0.31±0.29
Melt flow ratio (MFR)		unitless	120.5	90	130	68	51
SCR	ASTM 2019	hrs	800±90	>18000	3700±120	33000	25000
Tensile property	ASTM 2004	Cross machine direction					
Break stress	Type IV	kN/m	51±3	53±4	66±6.1	67±6.4	74±2.5
Break strain		%	860±23	980±92	890±72	960±104	1100±112
Break stress	Type V	kN/m	56 ±2.3	56±2.5	74±6	72± 7	59±3.1
Break strain		%	800±36	800±28	812±1	784±72	840±40

[a] Standard deviation; [b] Provided by GMB manufacturer; [c] Encapsulated. GMBs-Group 3 was used to investigate the effect of GMB's resin density on its resistance to degradation.

Table 1.d. Initial properties of GMBs- Group 4.

Property	Method	Unit	Mean ± SD[a]					
Designator	--	--	MxC15	MyF3-15	MzV20	MxV30	LxE15	LxV20
Type	--	--	HDPE	HDPE	HDPE	HDPE	LLDPE	LLDPE
Resin type	--	--	M2-1	M4	M2-2	M2-3	L1-2	L2
Manufacturing technique	--	--	Blown film	Flat die	Blown film	Blown film	Blown film	Blown film
Production date	--	--	2008	2013	2014	2014	2011	2014
Nominal thickness	ASTM 2012	mm	1.5	1.5	2.0	3.0	1.5	2.0
Resin density [b]	--	g/cm^3	0.936	0.933	Not supplied	0.937	Not supplied	0.919
GMB density [b]	ASTM 2010	g/cm^3	0.946	0.945	>0.941	0.943	Not supplied	0.934
Crystallinity [c]	ASTM 2018	%	56±1.8	51±1.4	53±2.2	54±1.2	36±1.3	41±0.8
Std-OIT	ASTM 2007	min	160±1.5	210±8	130 ± 6	250 ± 23	155 ± 5	200± 12
HP-OIT	ASTM 2006	min	960±17	1300±90	4600±160	1480 ± 8	890±25	4100±70
HLMI (21.6kg)	ASTM 2013	g/10min	13.9±0.8	17.3±0.3	11.9±0.6	13.4±0.6	14.7±0.25	14.62±0.6
LLMI (2.16 kg)		g/10min	0.115±0.003	0.74±0.044	0.094±0.004	0.17±0.01	0.153±0.011	0.31±0.29
Melt flow ratio (MFR)		unitless	120	26	130	80	90	51
SCR	ASTM 2019	hrs	800±90	6500±2200	3700±120	37000	>18000	25000
Tensile property	ASTM 2004	Cross machine direction						
Break stress	Type IV	kN/m	51 ± 2.7	59 ±1.5	66±6.1	110±3.4	53±3.8	74±2.5
Break strain		%	857 ± 23	960±10.4	890±72	1000±45	980±92	1100±112
Break stress	Type V	kN/m	56±2.3	56±2	74±6	110±7	56±2.5	59±3.1
Break strain		%	800±36	790±18	810±1	800±40	800±28	840±40

[a] Standard deviation; [b] Provided by GMB manufacturer; [c] Encapsulated. GMBs- Group 4 was used to investigate the effect of GMB's thickness on the longevity of GMBs in chlorinated water.

Table 2. Antioxidant depletion time, degradation of tensile properties in Stage (A), and time to severe degradation of the 12 GMBs immersed in chlorinated water (0.5 ppm free chlorine) at 85°C; rounded to 2 significant digits.

GMB	Std-OIT depletion time [months]	HP-OIT depletion time [months]	t_d[1] [months]	Normalized $F_{b\text{-}SO}$ (range of normalized $F_{b\text{-}SO}$) [unitless]	Normalized $\varepsilon_{b\text{-}SO}$ (range of normalized $\varepsilon_{b\text{-}SO}$) [unitless]	t_{sd} of tensile strength [months]	t_{sd} of break tensile strain [months]
MyF1-15	1.7	9.3	9.3	0.73 (0.56-0.93)	0.78 (0.48-0.95)	--	--
MyF2-15	2.5	8.2	8.2	0.64 (0.50-0.83)	0.70 (0.48-0.86)	--	--
LxE15	4.3	5.8	5.8	0.83 (0.61-0.95)	0.88 (0.71-1.0)	--	--
LxV20	4.4	11.8	11.8	0.84 (0.78-0.93)	0.90 (0.64-0.98)	--	--
BzV20	2.3	7.8	7.8	0.84 (0.63-0.94)	0.89 (0.71-0.97)	--	--
MxV30	7.5	5.7	7.5	0.81 (0.74-0.95)	0.87 (0.77-0.92)	--	--
MxC15[2]	1.9	6.6	6.6	0.70 (0.52-0.77)	0.66 (0.56-0.79)	67[2]	66[2]
MzV20	2.1	4.8	4.8	0.66 (0.48-0.83)	0.73 (0.54-0.89)	--	--
MyEW15	1.9	4.0	4.0	0.68 (0.56-0.94)	0.79 (0.61-0.89)	16 (<0.17)[3]	15 (0.08)[3]
MyF3-15	3.3	7.0	7	0.75 (0.63-0.96)	0.90 (0.65-1.02)	23(0.24)[4]	22 (0.06)[4]
MyE15	2.0	4.7	4.7	0.73 (0.61-0.88)	0.76 (0.60-0.85)	31[4](0.24)[5]	29[4] (0.24)[5]
LxD15	3.6	7.9	7.9	0.75 (0.61-0.93)	0.87 (0.67-0.93)	50[4] (0.45)[6]	49[4] (0.52)[6]

[1] Antioxidant depletion time estimated as the longer of Std-OIT or HP-OIT depletion time; [2] Abdelaal et al. (2019); [3] the number inside the parenthesis represents the $F_{b\text{-}SO}/\varepsilon_{b\text{-}SO}$ value at 14 months;[4] estimated by extrapolation of the data regression line in Stage (B). [5] the number inside the parenthesis represents the $F_{b\text{-}SO}/\varepsilon_{b\text{-}SO}$ value at 22 months; [6] the number inside the parenthesis represents the minimum $F_{b\text{-}SO}/\varepsilon_{b\text{-}SO}$ value at 35 months.

Table 3. Summary of Std-OIT results for 12 GMBs immersed in chlorinated water (0.5 ppm free chlorine) at 85°C.

GMB	Group	Type-thickness [mm]	*Std-OIT$_o$* [min]	Depletion rate [month^{-1}]	Time to depletion [months]	Residual Std-OIT value [min]	Relative initial Std-OIT[1]	Relative depletion time[2]
MyE15	1	HDPE-1.5	150±7	1.81	2.0	4±1	0.92	1.18
MyEW15		White HDPE1.5	170±5	2.36	1.9	2.1±0.4	1.06	1.12
LxD15		LLDPE-1.5	190±5	1.27	3.6	2±0.0	1.18	2.14
LxE15		LLDPE-1.5	155±5	0.88	4.3	3.5±0.7	0.96	2.58
MyF1-15	2	HDPE-1.5	160±5	2.7	1.7	1.7±0.3	1.00	1.00
MyF2-15		HDPE-1.5	190±3	2.5	2.5	1.4±0.4	1.16	1.48
MyF3-15		HDPE-1.5	210±8	1.96	3.3	2.5±1.1	1.30	1.98
MyE15		HDPE-1.5	150±7	1.81	2.0	4.1±1.1	0.92	1.18
LxD15		LLDPE-1.5	190±5	1.27	3.6	2.0±0.0	1.18	2.14
LxE15		LLDPE-1.5	155±5	0.88	4.2	3.5±0.7	0.96	2.58
MxC15[3]	3	HDPE-1.5	160±2	2.65	1.9	1.0±0.2	1.00	1.14
LxE15		LLDPE-1.5	155±5	0.88	4.3	3.5±0.7	0.96	2.58
MzV20		HDPE-2.0	130±6	1.48	2.1	4±2	0.80	1.38
BzV20		Blended-2.0	120±6	1.20	2.3	7±1.0	0.73	1.40
LxV20		LLDPE-2.0	200±12	0.84	4.4	4.8±1	1.24	2.66
MxC15[3]	4	HDPE-1.5	160±2	2.65	1.9	1.0±0.2	1.00	1.14
MyF3-15		HDPE-1.5	210±8	1.96	3.3	2.5±1	1.30	1.98
MzV20		HDPE-2.0	130±6	1.48	2.1	4.2±2	0.80	1.38
MxV30		HDPE-3.0	250±23	0.51	7.5	5.3±2	1.54	4.52
LxE15		LLDPE-1.5	155±5	0.88	4.3	3.5±0.7	0.96	2.58
LxV20		LLDPE-2.0	200±12	0.84	4.4	4.8±1	1.24	2.66

[1] The initial Std-OIT of the GMB divided by the initial Std-OIT of MyF1-15; [2] The depletion time of a certain GMB divided by the shortest depletion time among all GMBs; i.e. depletion time of MyF1-15; [3]Abdelaal et al. (2019).

Table 4. Summary of HP-OIT results for 12 GMBs immersed in chlorinated water (0.5 ppm free chlorine) at 85°C.

GMB	Group	Type-thickness [mm]	$HP\text{-}OIT_o$ [min]	Depletion rate [month^{-1}]	Time to depletion [months]	Residual HP-OIT value [min]	Normalized residual HP-OIT value [-]	Relative initial HP-OIT[1]	Relative depletion time[2]
MyE15	1	HDPE-1.5	1300±96	0.72	4.7	520±170	0.40±0.13	1.97	1.10
MyEW15		White HDPE-1.5	670±17	0.66	4.0	200±33	0.30±0.05	1.00	1.00
LxD15		LLDPE-1.5	350±13	0.49	7.9	25±5	0.07±0.02	0.52	1.82
LxE15		LLDPE-1.5	890±25	0.64	5.8	160±10	0.18±0.01	1.33	1.33
MyF1-15	2	HDPE-1.5	1100±110	0.38	9.3	350±25	0.32±0.02	1.62	2.14
MyF2-15		HDPE-1.5	780±62	0.39	8.2	400±39	0.51±0.05	1.16	1.90
MyF3-15		HDPE-1.5	1300±90	0.49	7.0	500±120	0.38±0.09	1.74	1.62
MyE15		HDPE-1.5	1300±100	0.72	4.7	520±170	0.39±0.13	1.97	1.10
LxD15		LLDPE-1.5	350±13	0.49	7.9	25±5	0.07±0.02	0.52	1.82
LxE15		LLDPE-1.5	890±25	0.64	5.8	160±10	0.18±0.01	1.33	1.33
MzV20	3	HDPE-2.0	4600±160	0.66	4.8	2400±260	0.53±0.06	6.90	1.11
BzV20		BPO-2.0	3700±400	0.38	7.8	2200±310	0.59±0.08	5.50	1.80
LxV20		LLDPE-2.0	4100±70	0.31	11.8	890±170	0.22±0.04	6.10	2.72
MxC15[3]		HDPE-1.5	960±17	0.48	6.6	510±37	0.53±0.04	1.44	1.52
LxE15		LLDPE-1.5	890±25	0.64	5.8	160±10	0.18±0.01	1.33	1.33
MzV20	4	HDPE-2.0	4600±160	0.66	4.8	2400±260	0.53±0.06	6.90	1.11
MxC15[4]		HDPE-1.5	960±17	0.48	6.6	510±37	0.53±0.04	1.44	1.52
MyF3-15		HDPE-1.5	1300±90	0.49	7.0	500±120	0.38±0.09	1.74	1.62
MxV30		HDPE-3.0	1480±8	0.56	5.7	780±110	0.53±0.07	2.22	1.31
LxE15		LLDPE-1.5	890±25	0.64	5.8	160±10	0.18±0.01	1.33	1.33
LxV20		LLDPE-2.0	4100±72	0.31	11.8	890±170	0.22±0.04	6.10	2.72

[1] The initial HP-OIT of the GMB divided by the initial HP-OIT of MyE15; [2] The HP-OIT depletion time of any GMB divided by the HP-OIT depletion of MyE15 whose the least antioxidant depletion time; [3] Abdelaal et al. (2019).

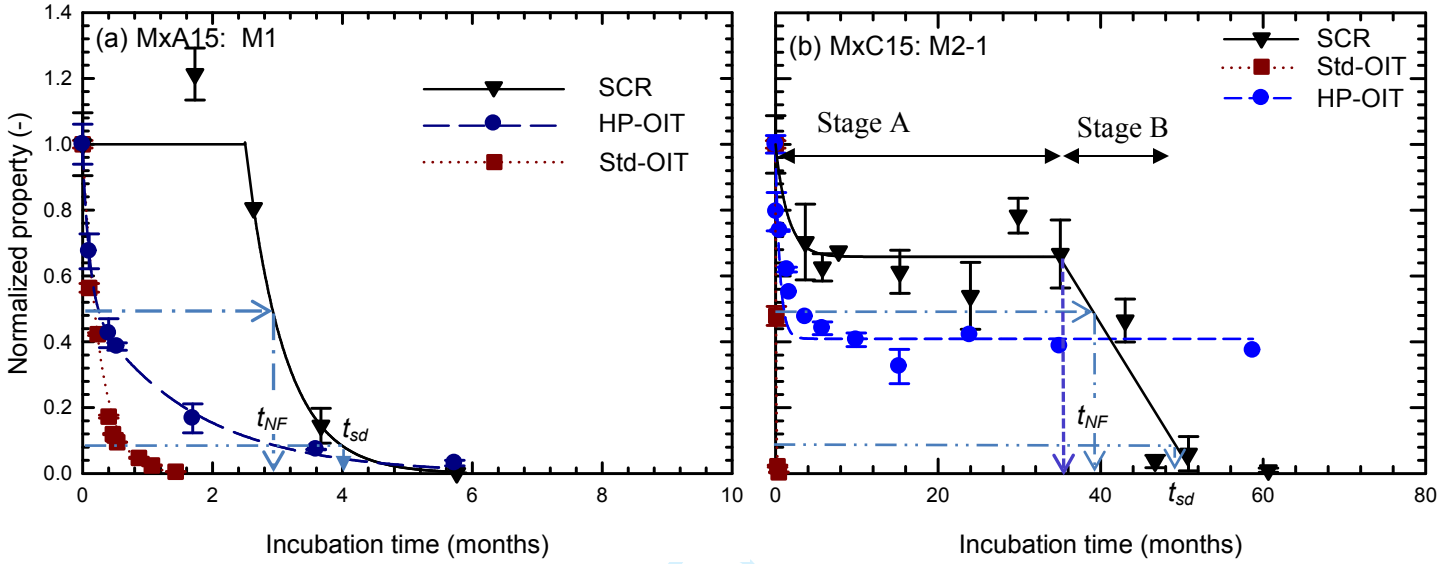

Figure 1. Variation of different index properties in chlorinated water (0.5 ppm free chlorine) at 85°C for: (a) MxA15 (without HALS; based on data published by Abdelaal and Rowe 2019) & (b) MxC15 (with HALS; based on data published by Abdelaal et al. 2019). t_{sd} = time to severe degradation and t_{NF} = time to nominal failure. Error bars represent range of results.

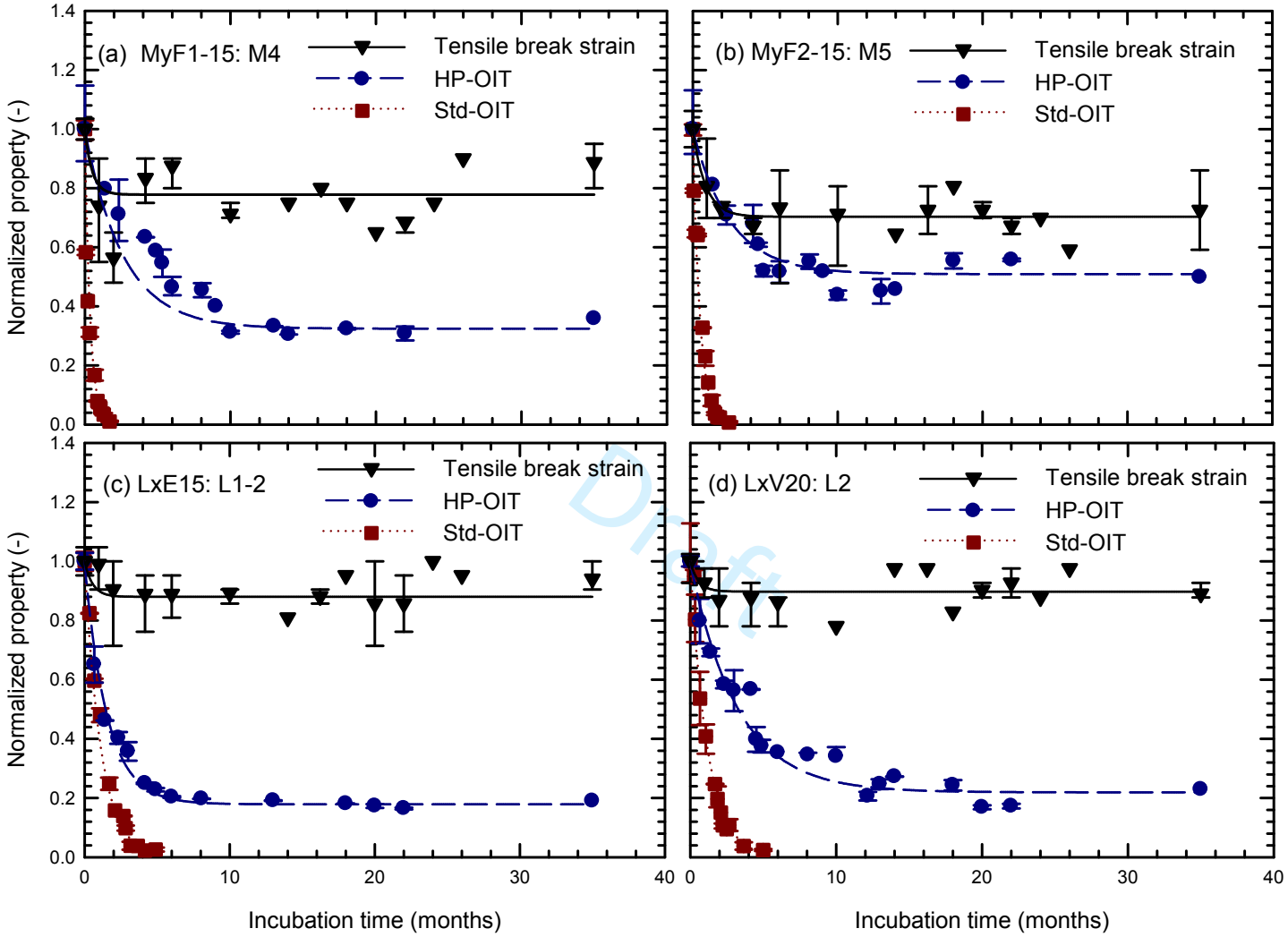
(a) MyF1-15: M4
(b) MyF2-15: M5
(c) LxE15: L1-2
(d) LxV20: L2
Tensile break strain
HP-OIT
Std-OIT
Normalized property (-)
Incubation time (months)
0.0
0.2
0.4
0.6
0.8
1.0
1.2
1.4
0
10
20
30
40

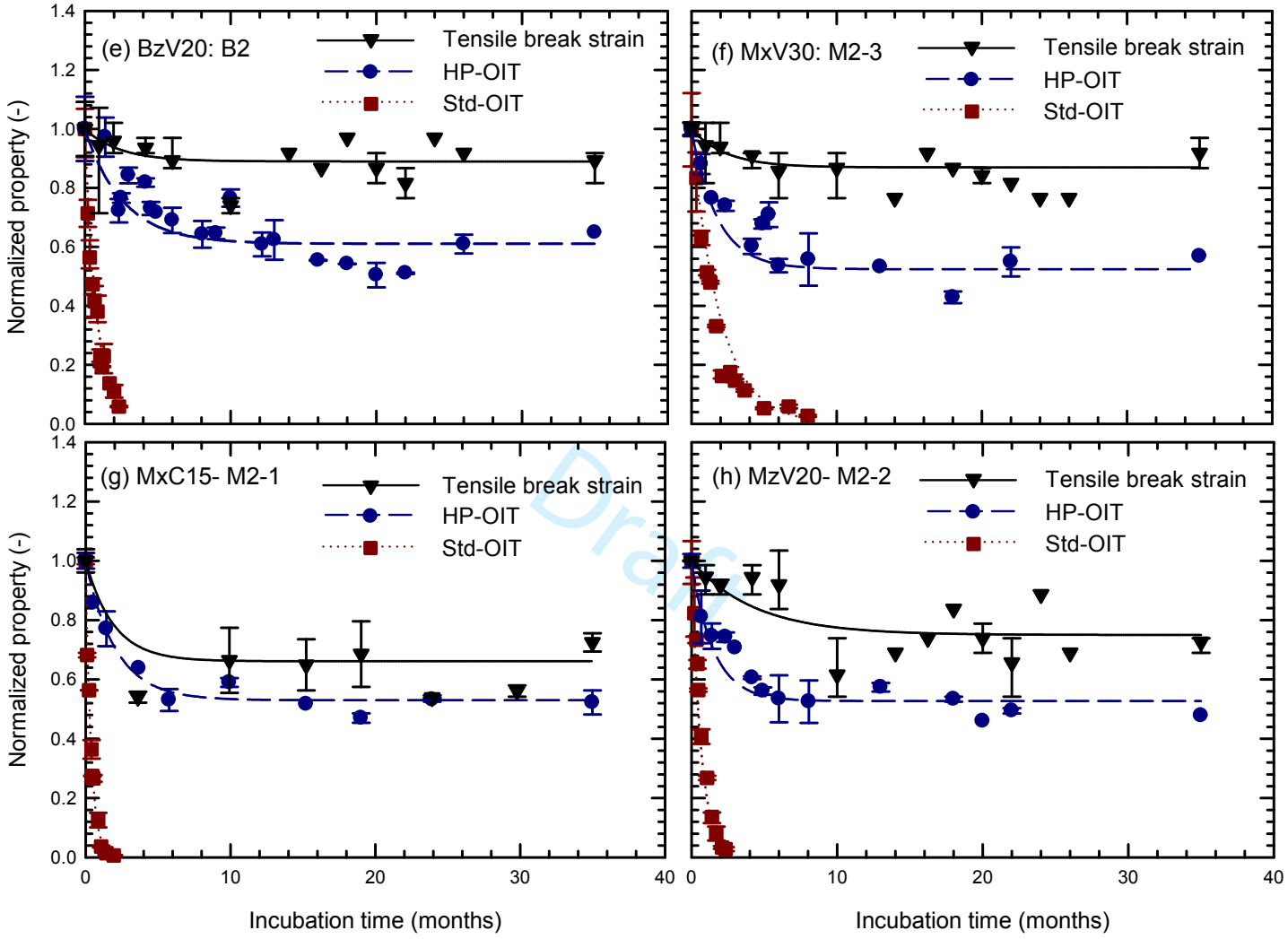
(e) BzV20: B2
(f) MxV30: M2-3
(g) MxC15- M2-1
(h) MzV20- M2-2
Tensile break strain
HP-OIT
Std-OIT
Normalized property (-)
Incubation time (months)
0.0
0.2
0.4
0.6
0.8
1.0
1.2
1.4
0
10
20
30
40

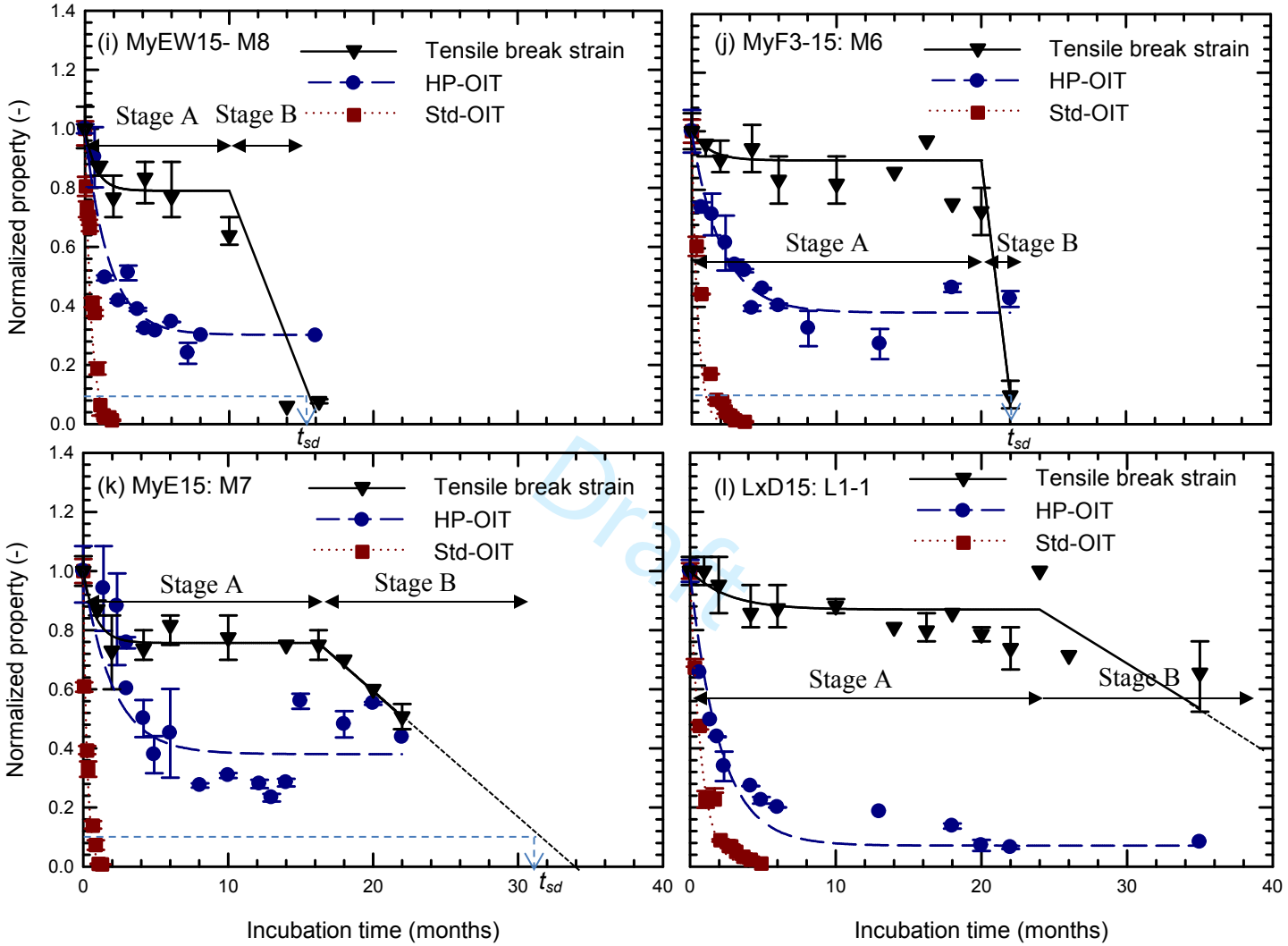

Figure 2. Degradation trends of 12 GMBs in chlorinated water (0.5 ppm free chlorine): (a) MyF1-15; (b) MyF2-15; (c) LxE15; (d) LxV20; (e) BzV20; (f) MxV30; (g) MxC15; (h) MzV20; (i) MyEW15; (j) MyF3-15; (k) MyE15; (l) LxD15. Error bars represent range of results.

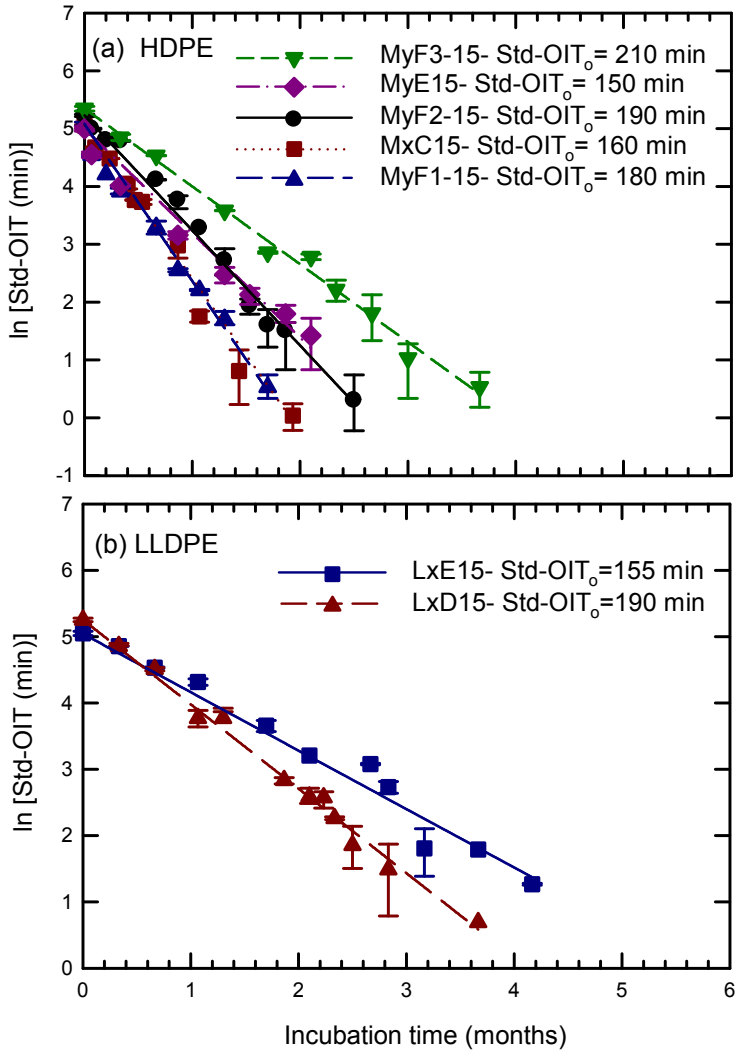

Figure 3. The effect of initial Std-OIT value on depletion time of 1.5 mm GMBs immersed in Chlorinated water (0.5 ppm free chlorine) at 85°C: (a) HDPE GMBs; (b) LLDPE GMBs. Error bars represent range of results.

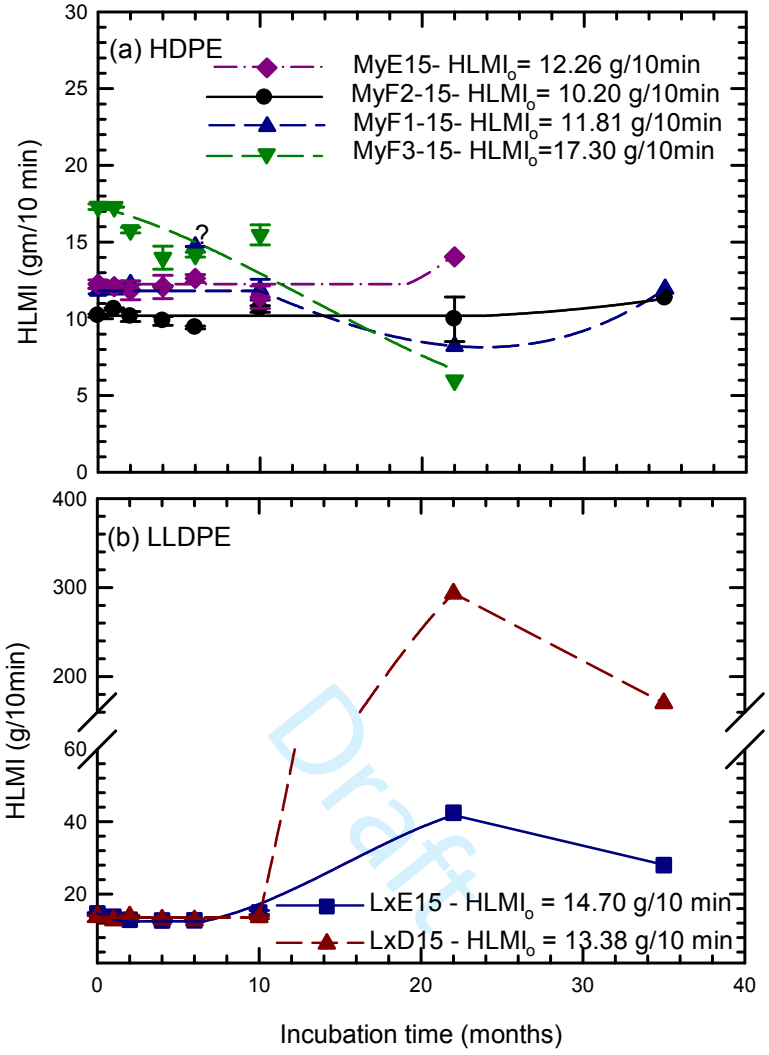

Figure 4. The effect of initial OIT value on MFI of 1.5 mm GMBs immersed in Chlorinated water (0.5 ppm free chlorine) at 85°C: (a) HDPE; (b) LLDPE. Error bars represent range of results. Last data point for MyE15 & MyF3-15 was 22 months because there was no enough GMB material for tensile & MFI tests at the time interval of 22-35 months. Data points marked by ("?") were excluded from interpretation.

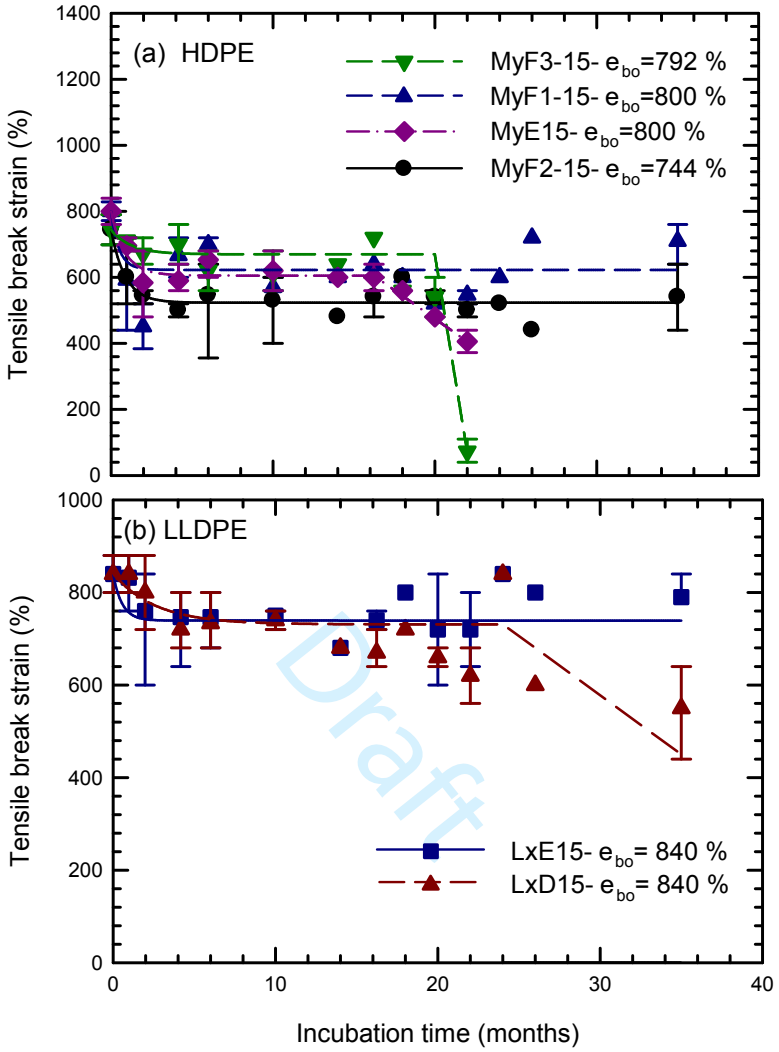

Figure 5. The effect of initial OIT value on degradation of tensile break strain with incubation time for 1.5 mm GMBs immersed in Chlorinated water (0.5 ppm free chlorine) at 85°C: (a) HDPE; (b) LLDPE. Error bars represent range of results. Last data point for MyE15 & MyF3-15 was 22 months because there was no enough GMB material for tensile & MFI tests at the time interval of 22-35 months.

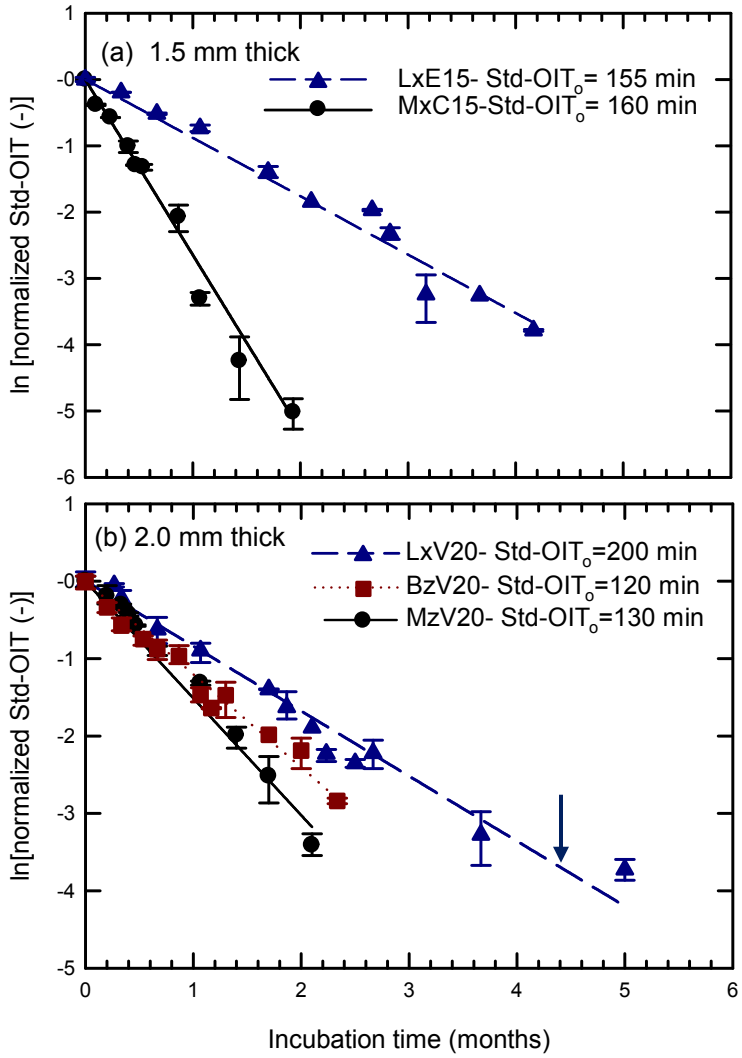

Figure 6. Variation of Std-OIT with incubation time in chlorinated water (0.5 ppm free chlorine) at 85°C for different GMB resin types: (a) 1.5 mm thick HDPE (MxC15) and LLDPE GMB (LxE15); (b) 2.0 mm thick HDPE (MzV20), LLDPE (LxV20), and BPO (BzV20) GMBs. The arrow indicates the antioxidant depletion time. Error bars represent range of results.

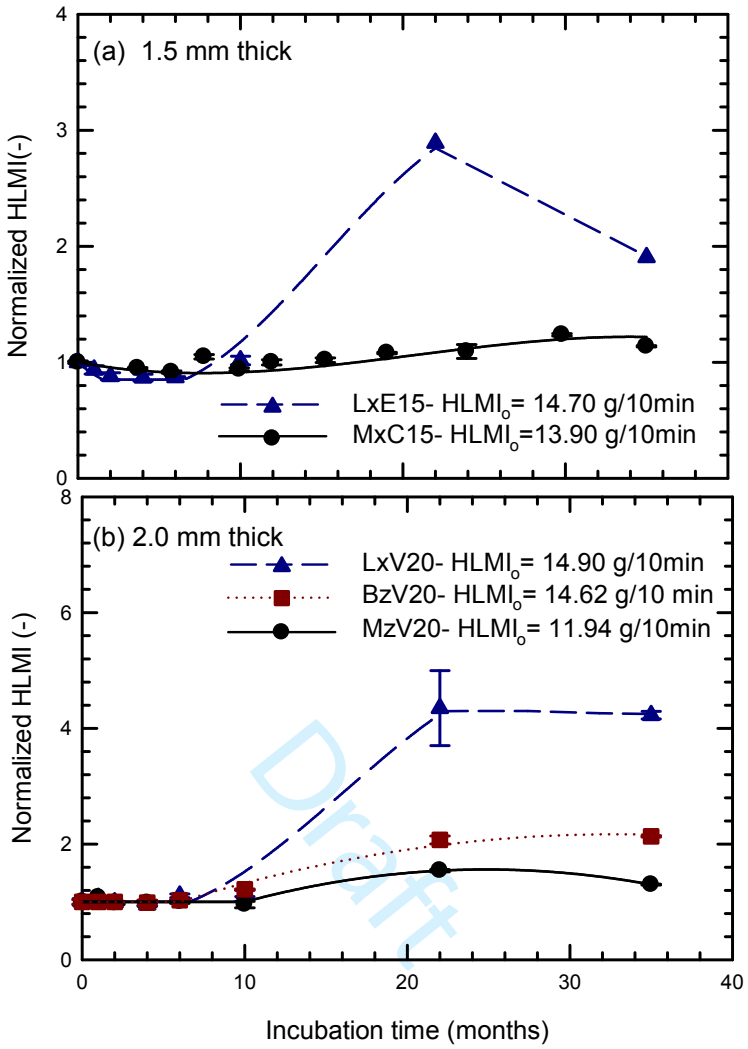

Figure 7. Comparison between changes in HLMI with incubation time for LLDPE, BPO, and HDPE GMBs immersed in Chlorinated water (0.5 ppm free chlorine) at 85°C: (a) 1.5 mm thick HDPE (MxC15) and LLDPE GMB (LxE15); and (b) 2.0 mm thick HDPE (MzV20), LLDPE (LxV20), and BPO (BzV20) GMBs. Error bars represent range of results.

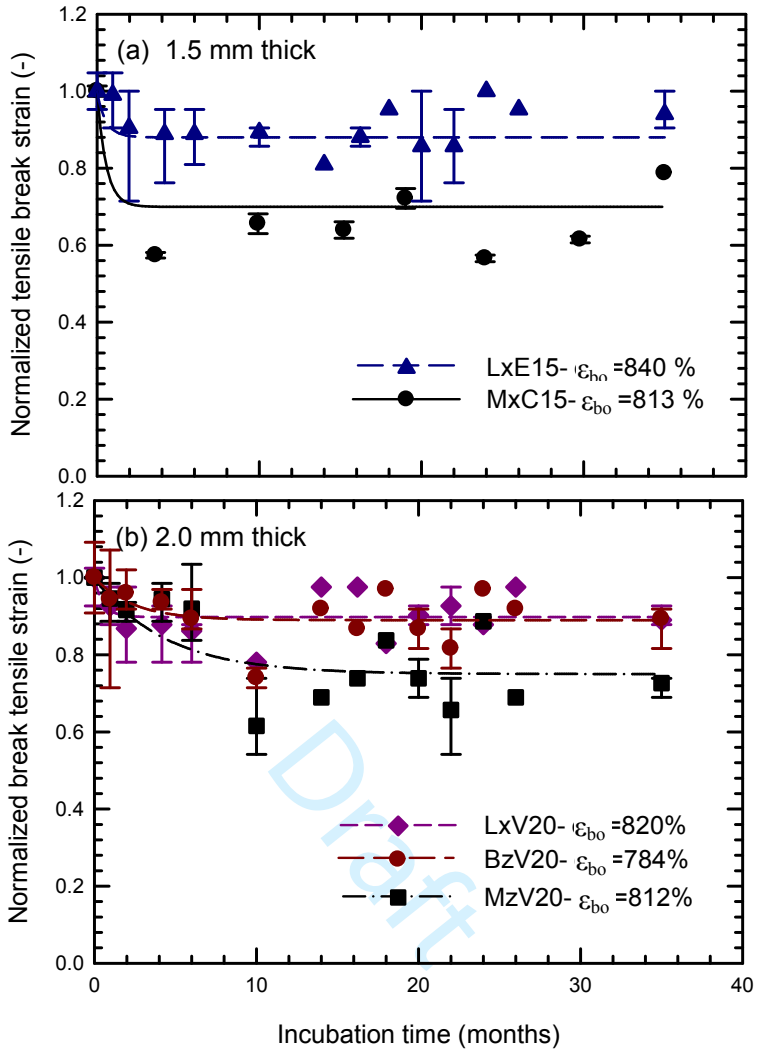

Figure 8. Comparison between degradation of physical properties with incubation time for LLDPE, BPO, and HDPE GMBs immersed in Chlorinated water (0.5 ppm free chlorine) at 85°C: (a) 1.5 mm thick HDPE (MxC15) and LLDPE GMB (LxE15); and (b) 2.0 mm thick HDPE (MzV20), LLDPE (LxV20), and BPO (BzV20) GMBs. Error bars represent range of results.

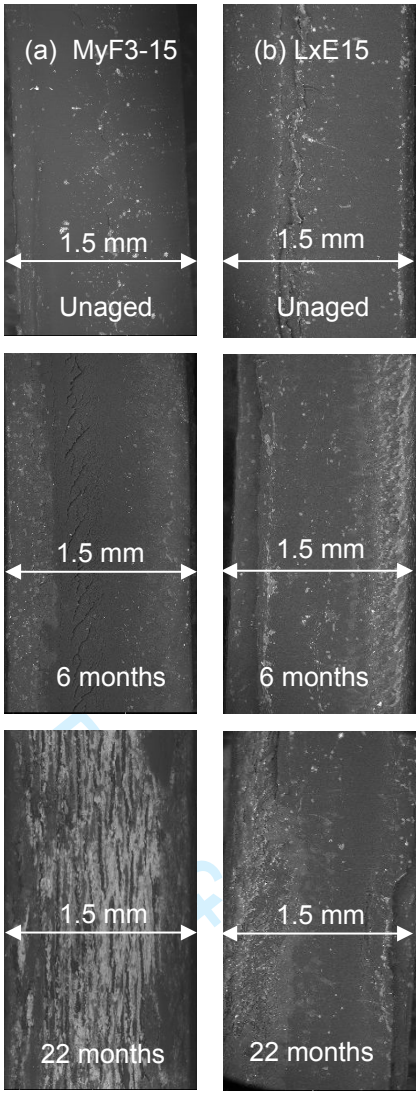

Figure 9. ESEM photos for GMBs incubated in chlorinated water (0.5 ppm free chlorine) at 85°C at different aging times of 0, 6, and 22 months: (a) MyF3-15, and (b) LxE15.

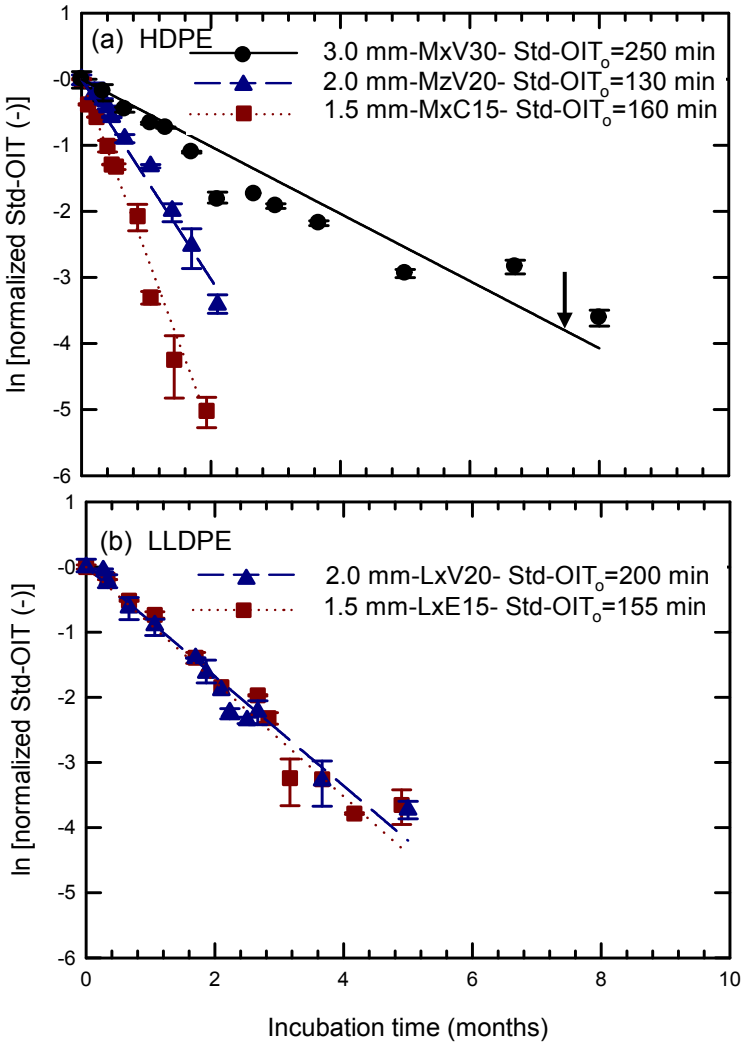

Figure 10. Variation of Std-OIT depletion with incubation time for GMBs of different thickness immersed in Chlorinated water (0.5 ppm free chlorine) at 85°C: (a) HDPE GMBs; and (b) LLDPE GMBs. The arrow indicates the antioxidant depletion time. Error bars represent range of results.

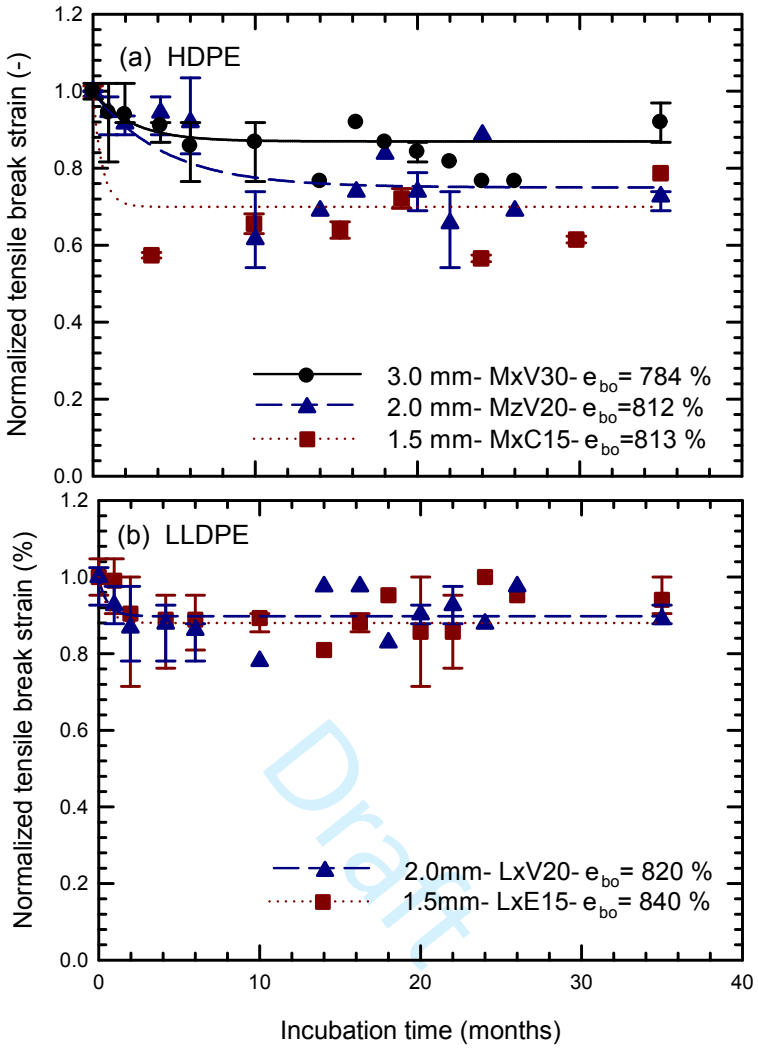

Figure 11. Variation of tensile break strain with incubation time for GMBs of different thickness immersed in Chlorinated water (0.5 ppm free chlorine) at 85°C: (a) HDPE GMBs; and (b) LLDPE GMBs. Error bars represent range of results.